JAGIELLONIAN UNIVERSITY
Marian Smoluchowski
INSTITUTE OF PHYSICS

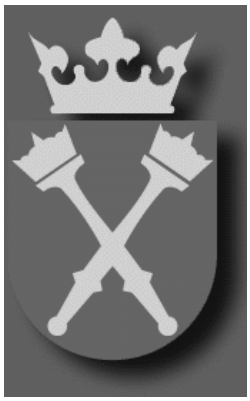

STRUCTURE OF DIFFERENTIALLY ROTATING BAROTROPES

Andrzej Odrzywołek

PhD Thesis

Supervisor:
Prof. Dr hab. M. Kutschera

CONTENTS

TABLES

FIGURES

Chapter 1

INTRODUCTION

1.1 Historical overview

Questions of the shape and the behaviour of celestial bodies intrigue human beings for many centuries. Ancient and medieval scientists believed that round shape of the Sun, Moon and Earth is one of the world principles and requires no further explanation. "Planets," as objects from eternal world, had to be of perfect shape – circle, ball etc. – as opposed to our imperfect environment. Galileo Galilei was one of the first men who realized, that the Moon, from general point of view, is an object similar to the Earth [9]. From this, and many other observations (Fig. 1.1), he correctly concluded, that entire universe is governed by the same principles as the Earth.

Nevertheless, Galileo Galilei had never asked why celestial bodies are round-shaped. As his predecessors, he assumed that perfect, round* shape is natural.

Following centuries brought new observations and theories. This had changed situation dramatically, leading to questions never asked before. Among them, some are still unanswered and subject of recent research.

The milestone of modern science, the Newton's theory of gravitation, was also essential to realize the existence of problems we consider in our thesis. It revealed the fact, that spherical shape of celestial bodies is just a direct consequence of gravitational attraction. This led to formulation of the essential term: *self-gravitating body*. Self-gravitating body is thus by definition the object bound together only by its own gravitational forces. Therefore, most of astronomical objects, in contrast to e.g. rocks bound by molecular forces, are self-gravitating. The shape of celestial bodies is then a result of physical laws. Fortunately, the simplest case of spherically symmetric solution is also the most frequent. Nevertheless, counterexamples of non-spherical bodies were found very early. The most intriguing was the mysterious shape of the planet Saturn. In 1659 Ch. Huygens determined the correct shape of Saturn as a planet surrounded by a thin disk not connected to the surface. Jupiter is also apparently flattened. Such observations indicated, that for some reason spherical shape is only approximation. Since Copernicus, we know the rotation of the Earth. Astronomical observations show rotation of other celestial bodies, and attempts were made to explain non-spherical shape by the influence of rotation.

Question then arises of the shape of rotating self-gravitating body. Isaac Newton discussed flattening of a rotating body due to balance of gravitational and centrifugal force at poles and

*From experiments, brilliant Galileo Galilei correctly deduced the law, nowadays referred to as "Galileo invariance." Free particles movement along straight lines, however, he treated as an approximation to the circular trajectories with some big radius! This clearly shows how difficult is to reject common ideas – here about special role of the circular orbits and ball shape.

Figure 1.1: Galileo, using the telescope made by himself found mountains and "seas" on the Moon. Therefore, celestial bodies are obviously of Earth-like nature. Nevertheless, his opponents refused to watch by any telescope, and thus he was forced to prove this to be true by other arguments [9]. One of them is result of the solar light reflecting analysis: perfectly smooth sphere reflects light (left) in obviously different manner (bright spot) than "imperfect" light scattering from irregular surface (right). Moon is resembling the latter case.

equator*.

First quantitative theory was given by Maclaurin in his book "*A Treatise of Fluxions*" printed in 1742. This was also one of the first applications for the Newton's new methods, referred to as infinitesimal calculus. He was able to find the shape of surface for uniformly rotating, homogeneous self-gravitating body. These ellipsoidal surfaces are referred to as Maclaurin spheroids.

In the 19-th century C. Jacobi investigated further this problem. He found a result, which importance was not realized even by himself. Namely, above some critical value (cf. APPENDIX D) we have the two possible configurations of equilibrium. One is a Maclaurin spheroid, the other is a triaxial ellipsoid. It shows, that three-dimensional solutions can be found even for apparently axially symmetric problem! From 20-th century physics point of view, we may say that Jacobi have found the first example of *spontaneous symmetry breaking*.

Progress made in late 19-th century and at the beginning of 20-th century led to many, but mostly negative results [19], e.g. regarding what is not solution of the rotating body problem (e.g. von Zeipel paradox [28]) or non-ellipticity of the surface [4]. Actually, solutions of a general case of compressible differentially rotating object with a free surface were unknown until development of numerical methods e.g. [7, 11, 24] and progress in computer hardware in 70's and 80's. Nowadays, the structure of rapidly rotating bodies can be investigated in non-stationary hydrodynamical situations [2, 16], of e.g. mass flows in binary stars [23].

Hopefully, in a near future we will be able to finally solve also outstanding problems of stellar rotation involving magnetic fields. At present however, we are still unable to compute fundamental properties of the rotating Sun**, to make quantitative prediction of a solar cycle period. Therefore development of simple analytical methods seems to be important for modelers to understand their own results. We would like to overview such well-known methods in the

*Ch. Huygens in 1690 also published important results for rotating body structure. Nevertheless, he never accepted Newton's theory of gravitation!

**The Sun is very slow rotator, compared to other stars.

next section.

1.2 Simple analytical formulae

Some of numerous analytical attempts to calculate the rotating body structure, such as the classic work of Maclaurin on ellipsoidal figures of equilibrium [20] and the Roche [17] model are

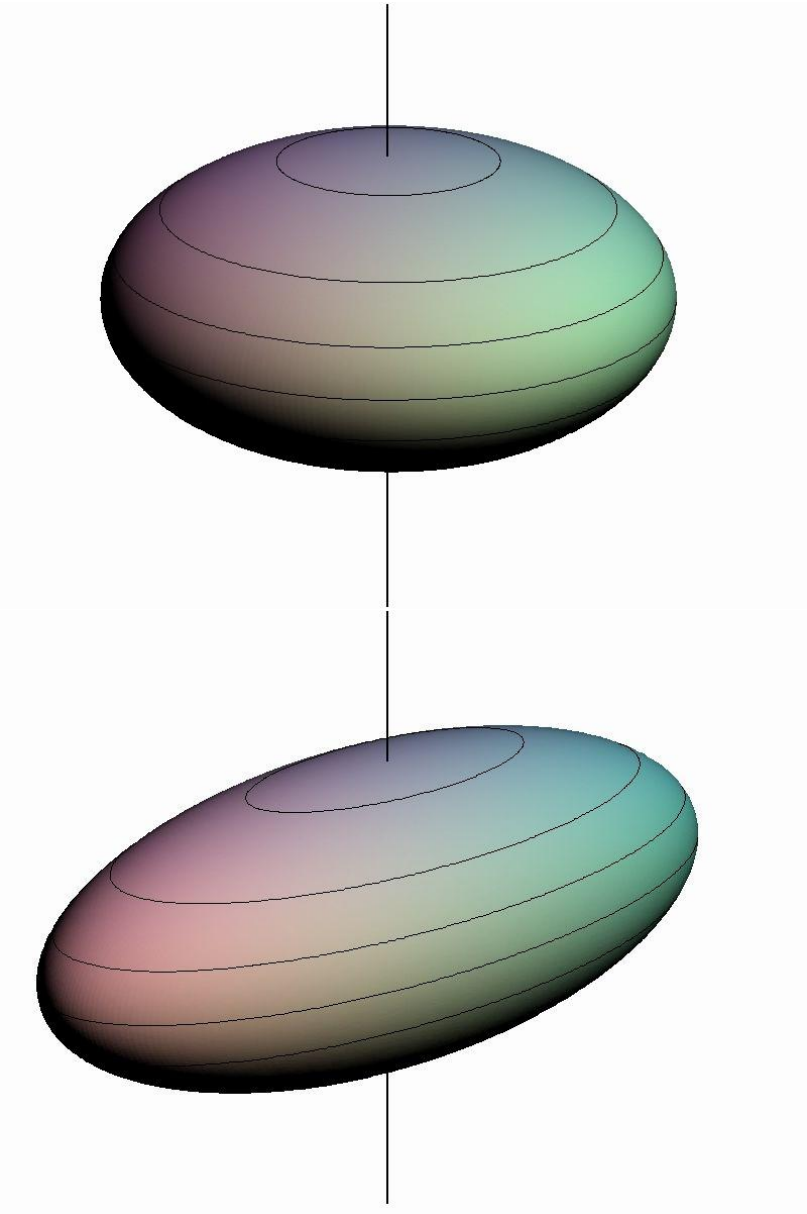

Figure 1.2: The Maclaurin spheroid (upper) and the Jacobi ellipsoid (lower) for kinetic to gravitational energy ratio $E_k/|E_g| = 0.1628$. Both of them are of the same mass, volume (due to constant density) and angular momentum. Difference in the shape is striking. The Jacobi ellipsoid is at the onset of the dynamical instability. Total mechanical energy of the Jacobi ellipsoid is smaller than that of the Maclaurin spheroid of the same angular momentum. Therefore, if some energy dissipation mechanism operates (e.g. viscosity, gravitational radiation) the Maclaurin spheroid will evolve towards triaxial shape. The figures are scaled properly according to physical properties, cf. APPENDIX D of [28].

still in use as excellent simple tools.

1.2.1 *Uniformly rotating homogeneous bodies*

One of the most important differences between the general rotating bodies and the uniform (homogeneous) ellipsoid with axes a_x, a_y, a_z is simple analytical form of gravitational potential in the latter case:

$$\Phi_g(x,y,z) = \pi\, G\, \rho \left[(a_x^2 - x^2)\, A_x + (a_y^2 - y^2)\, A_y + (a_z^2 - z^2)\, A_z \right]. \tag{1.1}$$

Expression above is valid for interior of the ellipsoid, and coefficients $A_i,\ i = x,y,z$ are, following [29], given by the formula:

$$A_i = a_x a_y a_z \int\limits_0^\infty \frac{du}{(a_i^2+u)(a_x^2+u)(a_y^2+u)(a_z^2+u)}. \tag{1.2}$$

According to e.g. our general equation (2.42) of rotating equilibrium discussed in detail later, at the surface ($h \equiv 0$) we have:

$$\Phi_g + \Phi_c = \pi\, G\, \rho \left[(a_x^2 - x^2)\, A_x + (a_y^2 - y^2)\, A_y + (a_z^2 - z^2)\, A_z \right] + \frac{1}{2}\Omega^2 \left(x^2 + y^2 \right) = C = const, \tag{1.3}$$

where we have used centrifugal potential Φ_c for rigid rotation (3.53), with z being the rotation axis. We may write the above equation in a standard form of the ellipsoidal surface:

$$\frac{x^2}{a_x^2} + \frac{y^2}{a_y^2} + \frac{z^2}{a_z^2} = 1, \tag{1.4}$$

with:

$$\frac{\widetilde{C}}{a_x^2} = \pi\, G\, \rho\, A_x - \frac{1}{2}\Omega^2, \tag{1.5a}$$

$$\frac{\widetilde{C}}{a_y^2} = \pi\, G\, \rho\, A_y - \frac{1}{2}\Omega^2, \tag{1.5b}$$

$$\frac{\widetilde{C}}{a_z^2} = \pi\, G\, \rho\, A_z, \tag{1.5c}$$

where:

$$\widetilde{C} = \pi\, G\, \rho \left(a_x^2 A_x + a_y^2 A_y + a_z^2 A_z \right) - C. \tag{1.5d}$$

Additionally, because our rotating body is incompressible, we have:

$$V = \frac{4}{3}\, \pi\, a_x a_y a_z. \tag{1.5e}$$

The system of equations (1.5) can be solved, giving the shape (i.e. a_x, a_y, a_z) of a rotating with angular velocity Ω body of volume V and density ρ. Solutions of eq. (1.5) are tabulated in Ref. [28]. There are two distinct types of rotating objects satisfying (1.5): axially symmetric Maclaurin spheroids ($a_x = a_y$) and genuine triaxial Jacobi ellipsoids ($a_x \neq a_y \neq a_z$). The axisymetric solution with $a_x = a_y$ is particularly easy to handle [20]. If we divide (1.5a) by (1.5c) and collect relevant terms we get:

$$\chi \equiv \frac{\Omega^2}{2\pi G \rho} = A_x - \frac{a_z^2}{a_x^2} A_z. \tag{1.6}$$

The integrals (1.2) can be expressed by elementary functions if $a_x = a_y$, and eq. (1.6) becomes:

$$\chi = \frac{\varepsilon(1+2\,\varepsilon^2)\arccos\varepsilon - 3\varepsilon^2\sqrt{1-\varepsilon^2}}{(1-\varepsilon^2)^{3/2}} \tag{1.7}$$

where $\varepsilon = a_z/a_x$ is the axis ratio. Dimensionless parameter χ is widely used to describe the rotation strength. Triaxial solutions do not appear until rotational kinetic to gravitational energy ratio $E_k/|E_g|$ exceeds the value of 0.1375, i.e. $\chi = 0.187$.

1.2.2 *Roche model*

In the Roche model we approximate gravitational force by a point-mass potential*:

$$\Phi_g(\mathbf{r}) = -G\,\frac{M}{\sqrt{r^2+z^2}}. \tag{1.8}$$

At the surface of the body we have:

$$\frac{GM}{\sqrt{r^2+z^2}} + \frac{1}{2}\Omega^2 r^2 = const = \frac{GM}{R_p}, \tag{1.9}$$

where R_p is the polar radius. From the condition of balance between centrifugal and gravitational forces at the equator, $GM/R_e^2 = R_e\,\Omega^2$, we get the maximum equatorial radius:

$$R_e = \sqrt[3]{\frac{GM}{\Omega^2}}. \tag{1.10}$$

Therefore, if centrally condensed body of mass M and equatorial radius R_e rotates faster than:

$$\chi = \frac{\Omega^2}{2\pi G\bar{\rho}} = \frac{V}{2\pi R_e^3} < \frac{\frac{4}{3}\pi R_e^3}{2\pi R_e^3} = \frac{2}{3} \tag{1.11}$$

where $\bar{\rho} = M/V$ is the mean density, then matter will be lost from the equator due to the centrifugal force. This estimate is based on the assumption that the volume of flattened due to rotation body can not exceed the volume of a ball with the radius R_e. More detailed calculations of a volume bounded by the critical surface give better estimate $\chi < 0.36$ [17].

1.2.3 *The postulate: need of simple models*

Two simple models mentioned in previous subsections represent limiting cases of possible rotating configurations: (1) a uniform body of constant density and (2) a centrally condensed body where almost the entire mass is concentrated at one point surrounded by essentially a weightless rotating envelope. Both of them are widely quoted in various context [22]. We can find them in many textbooks [17, 29, 28] as they are valuable educational tools. In contrast, methods developed for compressible bodies are quite complicated (e.g. Claiaraut-Legendere expansion in [28]), therefore not very useful.

In this thesis we propose simple analytical formula for compressible differentially rotating barotropes which is able to produce sensible results for a wide range of parameters. This formula can immediately give us approximate structure of rotating polytropes without involving numerical computations. All we need is some basic algebra and knowledge of the Lane-Emden functions.

*In cylindrical coordinates, cf. footnote on page 18; z is rotation axis.

Section 1.2

Chapter 2

BASIC EQUATIONS & FORMULAE

2.1 Derivation of basic equations

Our goal is to find the mechanical equilibrium of self-gravitating body of simple composition, assumed to be well approximated by the barotropic Equation Of State (thereafter EOS):

$$p = p(\rho). \tag{2.1}$$

Moreover, we neglect all effects related to viscosity, magnetic fields, general relativity corrections, tidal forces etc. However, even under these numerous simplifying assumptions, we are still unable to answer significant questions about properties of rotating body as e.g. if strong meridional circulation may affect global mechanical equilibrium. But this model is not trivial, as e.g. white dwarfs almost perfectly fit into this class of objects.

We will derive equations of the problem from basic physical principles. This simple derivation is relevant to our goal, but omits many important properties and problems related to stellar gas-dynamics. Reader interested in properties of much more general rotating stellar objects is referred to excellent textbooks of Tassoul [28, 29], and references therein. Fluid dynamics in general is covered by e.g. [18].

2.1.1 *Second Newton's law for fluid element*

Let us consider a small* fluid element of volume $\widetilde{V}$. From the second Newton's law $\mathbf{F} = m\mathbf{a}$, the force acting on the element is equal to the acceleration multiplied by the mass of the element:

$$\rho\widetilde{V}\,\frac{d\mathbf{v}}{dt} = \rho\widetilde{V}\,\mathbf{g} - \int\limits_S p\,d\mathbf{S} \tag{2.2}$$

where ρ is density of the element, and $\rho\widetilde{V}$ is the mass. The term $\rho\widetilde{V}\,\mathbf{g}$, where $\mathbf{g}$ is gravitational acceleration, is the gravitational force acting on the element, and the remaining term represents the force of external pressure.

We are going to eliminate $\widetilde{V}$ from (2.2). Let us multiply the last term in 2.2 by an arbitrary constant vector $\mathbf{k}$:

$$\mathbf{F}_p \cdot \mathbf{k} = -\left(\int\limits_S p\,d\mathbf{S}\right)\cdot\mathbf{k} \tag{2.3}$$

*As usual in fluid mechanics, we assume that fluid element is small compared to typical scale of problem, but still contain huge number of particles, so we can treat medium as a continuum.

where we have denoted pressure force by $\mathbf{F}_p$. The right hand side of the above equation is equal to:

$$\left(\int\limits_S p\, d\mathbf{S}\right)\cdot\mathbf{k} = \int\limits_S p\,\mathbf{k}\cdot d\mathbf{S} = \int\limits_{\widetilde{V}} \mathrm{div}(p\,\mathbf{k})\, dV = \int\limits_{\widetilde{V}} (\mathbf{k}\cdot \mathrm{grad}p + p\,\mathrm{div}\mathbf{k})\, dV.$$

Because divergence of constant vector $\mathbf{k}$ is equal to zero, we get:

$$\mathbf{F}_p\cdot\mathbf{k} = -\left(\int\limits_{\widetilde{V}} \mathrm{grad}p\, dV\right)\cdot\mathbf{k}. \tag{2.4}$$

This is true for any vector $\mathbf{k}$, so:

$$\mathbf{F}_p = -\int\limits_{\widetilde{V}} \mathrm{grad}\, p\; dV. \tag{2.5}$$

Volume $\tilde{V}$ is very small, and the integral can be replaced simply by

$$\mathbf{F}_p = -\,\widetilde{V}\;\mathrm{grad}\, p. \tag{2.6}$$

We thus managed to eliminate the volume $\widetilde{V}$ from eq. (2.2) which becomes

$$\rho\widetilde{V}\,\frac{d\mathbf{v}}{dt} = \rho\widetilde{V}\,\mathbf{g} - \widetilde{V}\;\mathrm{grad}\, p, \tag{2.7}$$

and, finally, the second Newton's law for fluid element is:

$$\rho\,\frac{d\mathbf{v}}{dt} = \rho\,\mathbf{g} - \mathrm{grad}\, p. \tag{2.8}$$

2.1.2 *Material derivative*

Equation (2.8) allows us to track particles moving in fluid. This approach (so-called Lagrangian coordinates) is not relevant to our problem of differential rotation*. Eulerian approach, where velocity, density and pressure fields are functions of time and space variables in fixed coordinate system will be used here. Transformation from Lagrangian coordinates (2.8) to Eulerian ones is made by substitution of the so-called material derivative of velocity field instead of acceleration:

$$\frac{d\mathbf{v}}{dt} \longrightarrow \frac{D\mathbf{v}}{Dt}. \tag{2.9}$$

Material derivative may be derived from a simple ,,rule of thumb" producing the correct result. Let $\mathbf{v}$ be a function of time t and Cartesian coordinates (x, y, z). We may write:

$$\frac{D\mathbf{v}}{Dt} = \frac{\partial\mathbf{v}}{\partial t}\frac{dt}{dt} + \frac{\partial\mathbf{v}}{\partial x}\frac{dx}{dt} + \frac{\partial\mathbf{v}}{\partial y}\frac{dy}{dt} + \frac{\partial\mathbf{v}}{\partial z}\frac{dz}{dt}.$$

*Let us imagine a star which is rotating faster at the center. After some time fluid elements near the center do more revolutions compared to the outer part of a body. Therefore, trajectories of fluid elements become progressively more twisted with time. In contrast, fixed in space, Eulerian coordinates are also constant with time.

Using $dx/dt = v_x, dy/dt = v_y, dz/dt = v_z$ we get:

$$\frac{D\mathbf{v}}{Dt} = \frac{\partial \mathbf{v}}{\partial t} + v_x \frac{\partial \mathbf{v}}{\partial x} + v_y \frac{\partial \mathbf{v}}{\partial y} + v_z \frac{\partial \mathbf{v}}{\partial z}$$

Introducing the operator:

$$\mathbf{v}\nabla \equiv (v_x \frac{\partial}{\partial x}, v_y \frac{\partial}{\partial y}, v_z \frac{\partial}{\partial z}) \tag{2.10}$$

we may write the material derivative in the usual form:

$$\frac{D\mathbf{v}}{Dt} = \frac{\partial \mathbf{v}}{\partial t} + \mathbf{v}\nabla \cdot \mathbf{v} \tag{2.11}$$

2.1.3 *Euler equation*

Finally, we get the Euler equation:

$$\frac{\partial \mathbf{v}}{\partial t} + \mathbf{v}\nabla \cdot \mathbf{v} = -\frac{1}{\rho} \operatorname{grad} p + \mathbf{g}. \tag{2.12}$$

In the equation of motion (2.12) we have the three unknown functions: the velocity field $\mathbf{v}$, the density ρ and the gravitational acceleration $\mathbf{g}$. Density is directly related to pressure p by the Equation Of State (2.1), so pressure is not additional independent quantity.

2.1.4 *Gravitational force*

In the Newton's theory of gravitation, acceleration $\mathbf{g}$ can be derived from the potential:

$$\mathbf{g} = -\operatorname{grad} \Phi_g. \tag{2.13}$$

The gravitational potential Φ_g satisfies the Poisson equation:

$$\Delta \Phi_g = 4\pi G \rho, \tag{2.14}$$

where $G = 6.672 \cdot 10^{-11}\, m^3 s^{-2} kg^{-1}$ is the gravitational constant, and $\rho = \rho(\mathbf{r})$ is, of course, density of matter.

2.1.5 *Continuity equation*

To close the system of basic equations we need the additional equation: the conservation of mass. Let us consider some volume V with boundary S. We may write:

$$\int_S \rho \mathbf{v} \cdot d\mathbf{S} = -\frac{\partial}{\partial t} \int_V \rho \, dV, \tag{2.15}$$

as a change of the total mass in the volume V is equal to flux of matter leaving V through the boundary surface S. Using the Gauss theorem we get:

$$\int_S \rho \mathbf{v} \cdot d\mathbf{S} = \int_V \operatorname{div}(\rho \mathbf{v}) \, dV. \tag{2.16}$$

Because the equation

$$\int_V \frac{\partial \rho}{\partial t} + \operatorname{div}(\rho \mathbf{v})\, dV = 0 \tag{2.17}$$

is fulfilled for any volume V the integrand must be identically equal to zero. This leads to a differential form of mass conservation: the continuity equation

$$\frac{\partial \rho}{\partial t} + \operatorname{div}(\rho \mathbf{v}) = 0. \tag{2.18}$$

2.1.6 *Complete system of basic equations*

The system of equations governing the motion of barotropic fluid consists of four (including EOS) equations:

$$\frac{\partial \mathbf{v}}{\partial t} + \mathbf{v}\nabla \cdot \mathbf{v} = -\frac{1}{\rho} \operatorname{grad} p - \operatorname{grad} \Phi_g, \tag{2.19a}$$

$$\Delta \Phi_g = 4\pi G \rho, \tag{2.19b}$$

$$\frac{\partial \rho}{\partial t} + \operatorname{div}(\rho \mathbf{v}) = 0, \tag{2.19c}$$

$$p = p(\rho). \tag{2.19d}$$

We are going to use equations (2.19) in case of a rotating star. Typically, we prescribe EOS and the velocity field in some analytical form, and the continuity equation becomes fulfilled automatically. Therefore, only two first equations in (2.19) are of particular interest in that case.

The above derivation tells us nothing about physical situations where barotropic EOS (2.1) is relevant. To know this derivation in a more general form, and discussion of specific cases is required. Particularly, (2.19) omit the problem of energy conservation and energy transport. Stars are objects producing energy, thus applications of the (2.19) to stars are limited. If, for example, we prescribe angular velocity profile $\Omega = \Omega(r, z)$ in a star, we may be unable to find the solution to energy transport equation. This is so-called von Zeipel paradox. Many authors [29] thus quote objects governed by the system of equations (2.19) as “stars,” in opposition to true stars, without quotes (“ ”). Nevertheless, if we are interested in mechanical equilibrium (not thermal equilibrium), the structure resulting from (2.19) may be a very good approximation. Moreover, objects not producing energy, described by the barotropic EOS (2.1) do exist. Namely, cold white dwarfs are perfectly described by eqs. (2.19). We can now move on with solving (2.19) in particular cases.

2.2 Equations of rotating self-gravitating body

Equations (2.19), of course, are much more general than we need, and govern all possible dynamical situations. Therefore, we now restrict (2.19) accordingly to the problem of rotating self-gravitating single body, floating freely in space.

2.2.1 *Stationary solution for isolated body*

Equations of fluid motion (2.19) govern any possible dynamical situation involving barotropic fluid with Newtonian gravity. To discuss a particular case of rotation we have to make some restrictive assumptions. First, it is safe to asssume that all quantities are time-independent

$$\frac{\partial \mathbf{v}}{\partial t} = 0, \qquad \frac{\partial \rho}{\partial t} = 0. \tag{2.20}$$

Let us note that this assumption does not describe a static situation, because velocity field is non-zero. Trivial example of such a motion is defined by constant velocity field. Physically, such velocity field describes motion of the entire considered object. Such motion does not influence the physical properties so we may require:

$$\int_V \rho \mathbf{v}\, dV = 0, \tag{2.21}$$

i.e. the total linear momentum is equal to zero. Simply speaking, we will consider stars at rest.

2.2.2 *Hydrostatic equilibrium*

The case $\mathbf{v} = 0$ describes the hydrostatic equilibrium:

$$\frac{1}{\rho}\,\mathrm{grad}\, p = -\mathrm{grad}\,\Phi_g. \tag{2.22}$$

For self-gravitating body the outer surface of a star is a sphere of radius, say R_0, and its density distribution is spherically symmetric. This is in great contrast to case of a rotating star, where the surface may be any function (in spherical coordinates $R = R(\theta, \phi)$) which is unknown *a priori*. This introduces serious problems, e.g. setting of boundary conditions for Poison equation becomes extremely difficult, as we do not know boundary surface. Only for simplest cases of uniform rotation, we are able to prove ellipsoidal shape of the boundary. In general it is impossible to say anything more than the object is somewhat flattened due to centrifugal force.

2.2.3 *Bernoulli's law*

If $\mathbf{v} \neq 0$ and $\partial \mathbf{v}/\partial t = 0$, the Euler equation (2.12) becomes:

$$\mathbf{v}\nabla \cdot \mathbf{v} = -\frac{1}{\rho}\,\mathrm{grad}\, p - \mathrm{grad}\,\Phi_g \tag{2.23}$$

We can write this equation in a more convenient form. First, let us introduce the enthalpy h:

$$h(\rho) = \int \frac{1}{\rho}\, dp. \tag{2.24}$$

Because $p = p(\rho)$, we may write:

$$\nabla h(p) = \frac{\partial h}{\partial p}\nabla p = \frac{\partial}{\partial p}\left(\int \frac{1}{\rho}\, dp\right) \nabla p = \frac{1}{\rho}\,\nabla p. \tag{2.25}$$

As we can see, the first term of the right-hand side of the Euler equation can be rewritten as:

$$\frac{1}{\rho}\,\nabla p \equiv \nabla h \tag{2.26}$$

To simplify the Euler equation further we use the identity:

$$\mathbf{v}\nabla \cdot \mathbf{v} = \frac{1}{2}\,\mathrm{grad}\, v^2 - \mathbf{v} \times \mathrm{rot}\mathbf{v} \tag{2.27}$$

Collecting all the gradient terms we get:

$$\nabla \left[h + \Phi_g + \frac{1}{2} v^2 \right] = \mathbf{v} \times \mathrm{rot} \mathbf{v}. \tag{2.28}$$

The above equation is sometimes referred to as Gromeka-Lamb equation. In case of $\mathbf{v} \times \mathrm{rot}\mathbf{v} = 0$ this leads to Bernoulli's equation:

$$h + \frac{1}{2} v^2 + \Phi_g = const \tag{2.29}$$

In rotating stars $\mathbf{v} \times \mathrm{rot}\, \mathbf{v} \neq 0$ but in particular cases it is possible to write equation very similar to Bernoulli's law. Actually, to obtain Bernoulli-like formula, we need only satisfy $\mathbf{v} \times \mathrm{rot}\, \mathbf{v} = \mathrm{grad}\, f$, where f is some function, and this is possible for so-called barotropic rotation law.

2.2.4 *Pure rotation*

To ensure that rotation is exclusive type of motion in our self-gravitating body, we may put:

$$\mathbf{v} = r\, \Omega(r, z)\, \mathbf{e}_\phi, \tag{2.30}$$

where cylindrical coordinates* (r, z, ϕ) were used. Here Ω is angular velocity. The motion defined by (2.30) is referred to as simple rotation, pure rotation or permanent rotation.

2.2.5 *Centrifugal force*

Substitution of the velocity field (2.30) into the Euler equation (2.12) leads to the following formula:

$$r\, \Omega(r, z)^2\, \mathbf{e}_r = \frac{1}{\rho} \mathrm{grad}\, p + \mathrm{grad}\, \Phi_c. \tag{2.31}$$

The equation above differs from the equation of hydrostatic equilibrium (2.22) only by the term

$$\mathbf{a}_c = -\, r\, \Omega(r, z)^2\, \mathbf{e}_r. \tag{2.32}$$

We identify this term with the centrifugal acceleration. This is a result we should expect for a rotating star.

2.2.6 *Poincaré-Wavre theorem*

Up to now, we have presumed that the angular velocity Ω may be any function of variables r and z: $\Omega = \Omega(r, z)$. This is not true, and it can be seen as follow. Let us take the curl ($\nabla\times$) of eq. (2.28):

$$\mathrm{rot}(\mathbf{v} \times \mathrm{rot}\mathbf{v}) = 0 \tag{2.33}$$

The left-hand side of eq. (2.28) disappears due to $\mathrm{rot}\, \mathrm{grad}(\cdot) \equiv 0$ identity. Eq. (2.33) is very useful, because it involves the velocity field $\mathbf{v}$ only. This equation has to be satisfied by any

* If not explicitly specified, since now, we always use cylindrical coordinates. They are defined in the usual form: $x = r\, \cos\phi, y = r\, \sin\phi, z = z$, where (x, y, z) are Cartesian coordinates.

velocity satisfying also the Euler equation. So let us substitute our simple rotation law (2.30) into (2.33). After some algebra we get:

$$2\,r\,\Omega(r,z)\,\frac{\partial\Omega(r,z)}{\partial z}=0. \tag{2.34}$$

This equation can be satisfied only if $\Omega\equiv 0$ or $\Omega=\Omega(r)$. Former case is not interesting (no rotation), but the latter case is a very important result: for barotropic fluid the angular velocity has to be constant over family of cylinders. Such rotation law is also referred to as barotropic rotation law. This includes very important case $\Omega=const$: so-called uniform or rigid rotation.

This result is somewhat surprising, and has been formulated as Poincaré-Wavre theorem:

THEOREM I

We define effective gravity $\mathbf{G}$ *as a sum of gravitational and centrifugal acceleration:*

$$\mathbf{G}=\mathbf{g}+r\,\Omega(r,z)^2\,\mathbf{e}_r. \tag{2.35}$$

For self-gravitating body in a state of permanent rotation the four following statements are equivalent:

(i) *Angular velocity* Ω *is constant over cylinders* $\Omega=\Omega(r)$.

(ii) *Surfaces* $\rho=const$ *and* $p=const$ *coincide.*

(iii) *Effective gravity* $\mathbf{G}$ *can be derived from potential.*

(iv) *Effective gravity* $\mathbf{G}$ *is normal to surfaces* $\rho=const$.

As an example, we prove equivalence of (i) and (ii). The operator $\nabla\times$ acting on both sides of time-independent Euler equation, in form (2.23), after use of eq. (2.27) is:

$$\nabla\times\left[\frac{1}{\rho}\,\mathrm{grad}\,p+(\nabla\times\mathbf{v})\times\mathbf{v}\right]=0. \tag{2.36}$$

Using simple rotation velocity field (2.30), after some algebra we get:

$$2\,r\,\Omega\,\frac{\partial\Omega(r,z)}{\partial z}\,\mathbf{e}_\phi=\nabla\left(\frac{1}{\rho}\right)\times\nabla p. \tag{2.37}$$

Vectors $\mathbf{u}_\rho=\nabla(1/\rho)=-\rho^{-2}\,\nabla\rho$ and $\mathbf{u}_p=\nabla p$ are normal to surfaces $\rho=const$ and $p=const$, respectively. Thus, the expression:

$$\nabla\left(\frac{1}{\rho}\right)\times\nabla p=0 \tag{2.38}$$

is a mathematical formulation of the fact that surfaces $\rho=const$ and $p=const$ coincide. If $\Omega=\Omega(r)$, LHS of eq. (2.37) is equal to zero; if isobaric and isopycnic surfaces coincide, RHS of eq. (2.37) is equal to zero, and Ω has to be function of r only, what ends the proof.

It is very important to notice, that for barotropic EOS (2.1) pressure is function of density only, and RHS of eq. (2.37) is identically zero. That is why EOS (2.1) excludes non-cylindrical (pure) rotation, and "cylindrical" rotation law $\Omega=\Omega(r)$ is often referred to as *barotropic rotation law*.

2.2.7 *Equation for rotating body*

Point (iii) of Poincare-Wavre theorem is of great practical importance, because it allows us to simplify the rotating body equation (2.31). This provides a result similar to Bernoulli's formula (2.29).

Let us introduce *centrifugal potential* Φ_c:

$$\Phi_c(r) = -\int_0^r \tilde{r}\,\Omega(\tilde{r})^2\,d\tilde{r}. \tag{2.39}$$

We can easily see that:

$$\mathrm{grad}\,\Phi_c = -r\,\Omega^2\mathbf{e}_r, \tag{2.40}$$

i.e. the centrifugal force can be derived from potential. This is a direct consequence of the point (iii) of Poincaré-Wavre theorem, as the Newtonian gravitational force is potential.

Now, the equation (2.31) using centrifugal potential Φ_c defined above, and enthalpy (2.26) becomes:

$$\nabla\left[h + \Phi_g + \Phi_c\right] = 0, \tag{2.41}$$

or even simpler:

$$h(\rho) + \Phi_g + \Phi_c = C = const, \tag{2.42}$$

where C is an arbitrary constant. The eq. (2.42) is the most important form of the equation for rotating self-gravitating body. Using Poisson equation (2.14) we may get single equation for e.g. density ρ. Equation (2.42) is still very difficult to solve, but it is significant step forward as we now have only one equation to solve. However, we still do not know if the continuity equation (2.18) is fulfilled.

2.2.8 *Continuity equation & axial symmetry of the solution*

Now we examine properties of continuity equation in case of a rotating star. Let us substitute simple rotation (2.30) into eq. (2.18). We *do not assume* that density is time-independent, and use $\rho = \rho(r, z, \phi, t)$. Then we get:

$$\frac{\partial\rho}{\partial t} + \Omega(r,z)\,\frac{\partial\rho}{\partial\phi} = 0. \tag{2.43}$$

Fortunately, we can find exact analytical solution to the equation above, and the result is:

$$\rho(r, z, \phi, t) = \tilde{\rho}(r, z, \phi - \Omega t) \tag{2.44}$$

where $\tilde{\rho}(r, z, \zeta)$ is an arbitrary function of three variables. Substitution of function (2.44) into eq. (2.43) gives

$$\frac{\partial\tilde{\rho}}{\partial t} + \Omega\,\frac{\partial\tilde{\rho}}{\partial\phi} = -\Omega\frac{\partial\tilde{\rho}(r,z,\zeta)}{\partial\zeta} + \Omega\frac{\partial\tilde{\rho}(r,z,\zeta)}{\partial\zeta} \equiv 0. \tag{2.45}$$

This confirms that the solution is correct. It is a bit confusing, for density shows time dependence although velocity field (2.30) is not time-dependent.

Actually, such solutions are realized in reality as non-axisymmetric uniformly rotating bodies, e.g. Jacobi ellipsoids (cf. Fig. 1.2). Their time-dependence of density $\rho = \rho(t)$ is usually not relevant, because it can be easily eliminated using simple transformation to co-rotating frame of reference: $\tilde{\phi} = \phi - \Omega\,t$. Generally, this is impossible, because $\Omega \neq const$.

However, if we are looking for solutions where $\partial\rho/\partial t = 0$, from (2.44), we immediately get very important result: our star is axially symmetric*. We would like to point out, that non-axisymmetric static solutions are only possible for uniform rotation $\Omega = const$. Any "marriage" of "triaxial" (non-axisymmetric) structure with differential rotation leads to fully dynamical problem. Usually, rotation is faster at the center, and outer parts of "triaxial" body are "delayed" with respect to the core, forming structure similar to spiral arms. Such a behaviour is seen in many hydrodynamical simulations of the rotating bodies [26].

2.3 Summary of the rotating barotropes

The following picture of our problem emerges. Under the following assumptions:

- Our body is self-gravitating
- EOS is barotropic
- Pure rotation is the only movement allowed

we found the following properties of the solutions of Euler equations (2.19):

- Angular velocity is constant over cylinders
- Density distribution is axially symmetric and time-independent
- Density satisfies eq. (2.42)

The rotating object satisfying conditions listed above is referred to as *barotrope*. Objects which do not satisfy the Poincaré-Wavre theorem are referred to as *barocline*. Any attempt to solve the structure of differentially rotating barotropic stars has to concentrate on solving equation (2.42) of rotating body structure. Next chapter will provide an elegant and relatively simple approximate solution of that equation.

*Symmetry with respect to equatorial plane, intuitively obvious, is difficult to prove. Such a symmetry always exists if $\Omega = \Omega(r)$ cf. discussion of the Lichtenstein theorem in [28].

Chapter 3

ANALYTICAL APPROXIMATE METHOD FOR DIFFERENTIALLY ROTATING BAROTROPES

3.1 Dual nature of the rotating barotrope equation

In previous section we have derived equation which has to be satisfied by the density stratification in a rotating barotrope:

$$h(\rho) + \Phi_c + \Phi_g = C. \tag{3.1}$$

Centrifugal potential Φ_c is fixed and given by *a priori* defined angular velocity $\Omega(r)$. The constant value C is a free parameter. This parameter defines a family of solutions in similar manner as does the central density for non-rotating polytropes. In (3.1) we have the two unknown functions: the density ρ and the gravitational potential Φ_g. We still need an additional relation between the density and the gravitational potential. Such a relationship exists in Newtonian theory of gravitation. It can be formulated either in differential or integral form.

3.1.1 *Differential form of the equation*

Gravitational potential and density are related by means of Poisson equation. We then need to solve the following system of equations:

$$h(\rho) + \Phi_c + \Phi_g = C, \tag{3.2a}$$

$$\Delta\Phi_g = 4\pi G\,\rho. \tag{3.2b}$$

Eq. (3.2) can be written in the form of a single equation with one unknown function. Laplacian of eq. (3.1) allows for elimination of gravitational potential using the Poisson equation giving:

$$\frac{1}{\rho}\frac{\partial p}{\partial \rho}\,\Delta\rho + 4\pi G\,\rho + \Delta\Phi_c = 0. \tag{3.3}$$

This is non-linear, inhomogeneous, second-order, parabolic differential equation for the density distribution $\rho(r, z)$ in two dimensions. Major difficulty, however, is not related to the form of eq. (3.3), but arises when one attempts to fix boundary conditions for it. The shape of boundary (surface) of a rotating star is not an initial part of the problem, but it is one of the final results!

Unfortunately, in general case of compressible and differentially rotating body* surface may be any function of angle from the rotation axis.

This leads to serious problems. Analytic continuation into the complex plane, converting equation (3.3) into hyperbolic type was used by Eriguchi [7] to avoid these difficulties. Boundary problem can be replaced by initial-value problem, leading to powerful computational numerical method – so-called EFGH method [6, 8, 10].

3.1.2 *Integral equation form of the equation*

Difficulties with differential form of the basic equation for rotating body stimulated research on alternative methods. System of equations (3.2) may be written as well as:

$$h(\rho) + \Phi_c + \Phi_g = C, \tag{3.4a}$$

$$\Phi_g(\mathbf{r}) = -G \int \frac{\rho(\tilde{\mathbf{r}})}{|\mathbf{r} - \tilde{\mathbf{r}}|}\, d^3\tilde{\mathbf{r}}, \tag{3.4b}$$

where instead of the Poisson equation, we have used its formal integral solution. This immediately leads to *integral equation* of rotating self-gravitating body:

$$h(\rho) + \Phi_c - G \int \frac{\rho(\tilde{\mathbf{r}})}{|\mathbf{r} - \tilde{\mathbf{r}}|}\, d^3\tilde{\mathbf{r}} = C. \tag{3.5}$$

In this equation $\rho(\mathbf{r})$ is an unknown function we are solving for, $\Phi_c(\mathbf{r})$ and $h(\rho)$ are functions resulting from our astrophysical problem, and C is a free parameter. Centrifugal potential Φ_c is responsible for rotation, enthalpy $h(\rho)$ is defined by the EOS, and the parameter C defines family of solutions with the same rotation pattern and equation of state, but different total mass. The integral equation is essential to derive our approximate formula. We take a closer look at the properties of eq. (3.5).

3.2 Properties of the integral equation

3.2.1 *Integral operator* $\mathcal{R}$

We may write our equation in a concise form:

$$h(\rho) + \Phi_c + \mathcal{R}(\rho) = C, \tag{3.6}$$

where $\mathcal{R}$ is an integral operator acting on density, here in cylindrical coordinates (r, z, ϕ):

$$\mathcal{R}(\rho) \equiv -G \int_0^{R_{eq}} \int_{-R_s(r)}^{R_s(r)} \int_0^{2\pi} \frac{\rho(r', z')}{\sqrt{(r'\sin\phi' - r\sin\phi)^2 + (r'\cos\phi' - r\cos\phi)^2 + (z' - z)^2}}\, d^3\mathbf{r}'. \tag{3.7}$$

Here $d^3\mathbf{r}' = r' dr' dz' d\phi'$ is volume element. In (3.7) we have explicitly assumed axial symmetry (i.e. ρ does not depend on ϕ) and planar (with respect to $z = 0$ plane) symmetry, i.e. boundary surfaces below and above $z = 0$ are both described by the function $R_s(r)$; R_{eq} is the equatorial radius of a self-gravitating body. Integral operator $\mathcal{R}(\rho)$ gives gravitational potential Φ_g.

*Incompressible, uniformly rotating bodies possess ellipsoidal surface.

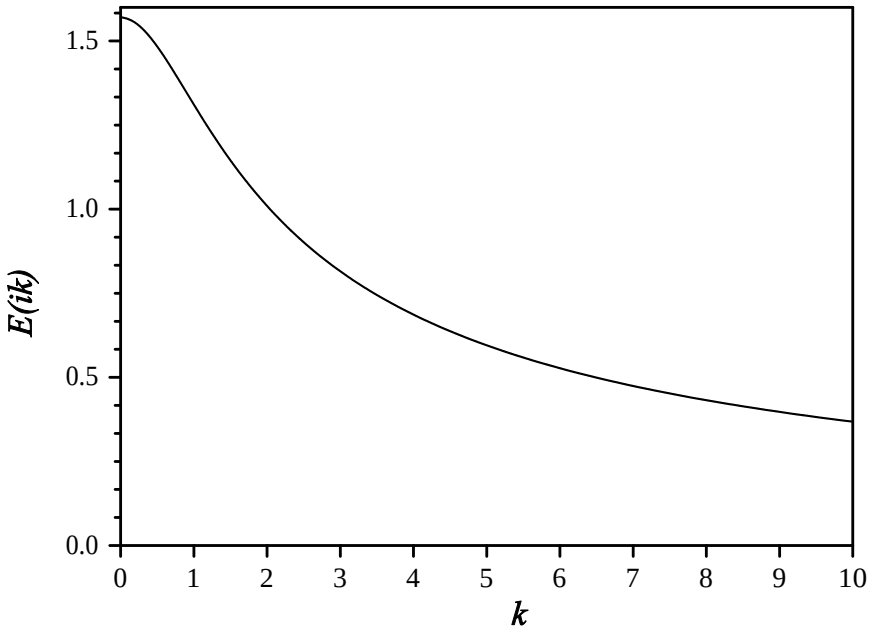

Figure 3.1: Complete elliptic integral of the first kind, E, for the imaginary argument $E(i\,k)$. $E(0) = \pi/2$, $\lim_{k\to\infty} E(i\,k) = 0$.

3.2.2 *Two-dimensional kernel*

Integration over variable ϕ in (3.7) can be made analytically*:

$$\int_0^{2\pi} \frac{d\phi'}{\sqrt{(r'\sin\phi' - r\sin\phi)^2 + (r'\cos\phi' - r\cos\phi)^2 + (z'-z)^2}} = \tag{3.8}$$

$$= 4\,\frac{E(ik)}{\sqrt{(r'-r)^2 + (z'-z)^2}},\ \text{where}: k^2 = \frac{4rr'}{(r'-r)^2 + (z'-z)^2}.$$

Function E is complete elliptic integral of the first kind [1]:

$$E(k) = \int_0^{\pi/2} \frac{1}{\sqrt{1 - k^2\sin^2\psi}}\,d\psi \tag{3.9}$$

If reader is confused by an imaginary number in the argument of the elliptic function (3.9), we note that if k is real and $k > 0$, then $E(ik)$ is real (Fig. 3.1). One can avoid the imaginary argument using e.g. the following identity:

$$E(ik) = \frac{1}{\sqrt{1+k^2}}\,E\left(\frac{k}{\sqrt{1+k^2}}\right) \tag{3.10}$$

Usage of the imaginary argument leads to somewhat shorter expression for the integral (3.9).

*Two definitions of elliptic integrals may be encountered, cf. APPENDIX C.

Our integral operator is now two-dimensional:

$$\mathcal{R}(\rho) \equiv -4G \int_{0}^{R_{eq}} \int_{-R_s(r)}^{R_s(r)} \frac{\rho(r^{'}, z^{'})\, r^{'} E(ik)}{\sqrt{(r^{'}-r)^2 + (z^{'}-z)^2}}\, dz^{'} dr^{'} \tag{3.11}$$

Reduction of integral dimension from three to two is natural for axisymmetric problem. It is also important from practical point of view, as computational time spent on calculating 2D integral is shorter compared to 3D integrals. Method presented above is an alternative to expansion of integrand in (3.9) into spherical harmonics series.

3.2.3 *Boundary conditions*

Actually, to derive our analytical formula explicit knowledge of integral operator $\mathcal{R}$ in terms of e.g. coordinates is not needed [21], but is very useful for clarifying many aspects of the problem.

For example, explicit form (3.11) of $\mathcal{R}$ suggests, that instead of a single unknown function $\rho(r, z)$, we have the two functions, including shape of the boundary surface $R_s(r)$. Let us examine this topic in detail.

If we prescribe some form of the function $R_s(r)$, and try to solve integral equation (3.5), then, from purely mathematical point of view, we could get some solution*. This solution, however, is likely to be unphysical, because physical solutions have to obey additional constraints: density has to be finite and $\rho(r, z) \geq 0$. Additionally, on the boundary surface, for gases we expect $\rho(r, z) = 0$. This strongly suggests introduction of additional equation connecting two unknown functions $\rho(r, z)$ and $R_s(r)$:

$$\rho\left(r, R_s(r)\right) = 0. \tag{3.12}$$

This gives integration limits in (3.11) as an implicit function, given by eq. (3.12).

In situations like described above, theory of integral equations commonly employs the following trick. Using the Heaviside (unit step) function:

$$\theta(x) = \begin{cases} 1 & \text{if } x \geq 0 \\ 0 & \text{if } x < 0 \end{cases}, \tag{3.13}$$

we may write the integral operator (3.11) as:

$$\mathcal{R}(\rho) \equiv -4G \iint_{A} \theta\left(\rho(r, z)\right) \frac{\rho(r^{'}, z^{'})\, r^{'} E(ik)}{\sqrt{(r^{'}-r)^2 + (z^{'}-z)^2}}\, dz^{'} dr^{'}, \tag{3.14}$$

where A denotes integration area. We assume only that A (usually of rectangular shape, cf. Fig. 3.2) is big enough to fit our rotating star inside. Using the form (3.14) we have the boundary conditions incorporated directly into integrand. As we can see, the integral form of our basic equation (2.42) overcome the problem of boundary surface and leave us with one integral equation (3.6) with one unknown function $\rho(r, z)$.

*If such a solution exists, what is not obvious, and is difficult to prove in our case of non-linear problem.

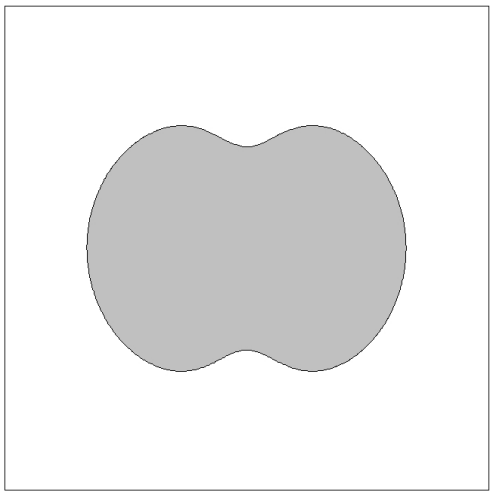

Figure 3.2: Shaded area defines the integration area for integral operator $\mathcal{R}$, in typical case of rotating body. Two methods exist for specification of that area: (1) introduction of a new function for boundary shape or (2) incorporating into integrand of $\mathcal{R}$ the unit step function $\theta(\rho)$. In the latter case we are integrating over fixed area of e.g. rectangular shape.

3.2.4 *Nonlinearity of integral equation*

Let us write again our integral equation:

$$h(\rho) + \Phi_c + \mathcal{R}(\rho) = C \tag{3.15}$$

where the integral operator is:

$$\mathcal{R}(\rho) = \iint\limits_A K(r, r^{'}, z, z^{'})\, \theta\left(\rho(r^{'}, z^{'})\right)\ \rho(r^{'}, z^{'})\, dr^{'} dz^{'}, \tag{3.16}$$

and the kernel K reads:

$$\mathrm{K}(r, r^{'}, z, z^{'}) = \frac{\rho(r^{'}, z^{'})\, r^{'} E(ik)}{\sqrt{(r^{'} - r)^2 + (z^{'} - z)^2}}\,, \quad k = \sqrt{\frac{4rr^{'}}{(r^{'} - r)^2 + (z^{'} - z)^2}}.$$

If the function $h(\rho)$ is non-linear, then the entire integral equation (3.15) is non-linear. Enthalpy $h(\rho)$ is a linear function only if the equation of state takes the form $p \sim \rho^2$, cf. (3.63), which is not particularly interesting case from physical point of view. Therefore almost all interesting cases are governed by non-linear enthalpy dependence on density.

We would like to point out, that from purely mathematical point of view, integral operator $\mathcal{R}$ (3.16) is also non-linear, due to presence of Heaviside function (3.13), which is obviously non-linear in general case. This seems to be contrary to well-known superposition rule for the gravitational potential. Actually, physical density is non-negative quantity, and indeed, if $\rho > 0$ then $\theta(\rho) = \rho$ is a linear function. In general, however, we are unable to avoid negative density at all steps of the solving procedure for equation (3.15). Fortunately, we do not want to satisfy

$\rho \geq 0$ for all steps leading to solution, but we only demand $\rho \geq 0$ for the final result. As we will see in the next sections, our approximate solution of eq. (3.15) is unable to produce accurate results, if we reject negative values of enthalpy for initial zeroth-order function.

3.2.5 *Canonical form of integral equation*

Equation (3.6) has a form of non-linear Hammerstein equation [12]. Actually, Hammerstein considered one-dimensional equations, but we also can use his transformation into canonical form [25]. Introducing new unknown function f:

$$f = C - \Phi_c - h(\rho), \tag{3.17}$$

and additional function F:

$$F(f) = h^{-1}(C - \Phi_c - f), \tag{3.18}$$

equation (3.6) becomes:

$$f = \mathcal{R}\left[F(f)\right]. \tag{3.19}$$

Closer look at equations (2.42) & (3.17) reveals the physical meaning of canonical unknown function f in the sense of Hammerstein. It is simply gravitational potential * Φ_g. Canonical form (3.19) allow us to find our approximate formula, as it is explained in the next section.

3.3 Derivation of the analytical formula

3.3.1 *Von Neumann series*

Derivation in this section is based on our article [21]. In section 3.1 we have discussed properties of the integral equation (3.6) for a rotating self-gravitating body. This equation has a form of the Hammerstein non-linear integral equation (3.19). Canonical form indicates the method of solving. For linear function F in (3.19), the equation could be easily solved by the von Neumann series (cf. APPENDIX A). This strongly suggests to try the following iteration scheme:

$$\begin{aligned} f_1 &= \mathcal{R}[F(f_0)], \\ f_2 &= \mathcal{R}[F(f_1)], \\ &\cdots \\ f_n &= \mathcal{R}[F(f_{n-1})] \\ &\cdots \end{aligned} \tag{3.20}$$

In case of general non-linear equation we are unable to prove convergence of the sequence (3.20). This can only be made for special cases e.g. the linear Fredholm equation (cf. APPENDIX A). Fortunately, it has been shown that the sequence (3.20) is convergent for a wide range of applications. An iteration procedure of this type was successfully applied in the self-consistent field method of Ostriker & Mark [24], in HSCF** [11] method and other. All of them are numerical methods. However, we have found very interesting analytical approximate solution of the integral equation (3.6) based on the iterative scheme (3.20).

*This is true only inside a star. Physical gravitational potential is well-defined for the entire space, while the function f is defined only for stellar interior.

**Hachisu Self-Consistent Field method.

3.3.2 *First term of the series*

First term of the sequence (3.20) is:

$$f_1 = \mathcal{R}\left[F(f_0)\right]. \tag{3.21}$$

Let calculate the right-hand side of the equation above. According to (3.18), $F(f_0)$ is:

$$F(f_0) = h^{-1}\left[C - f_0 - \Phi_c\right], \tag{3.22}$$

but, due to definition (3.17), $f_0 = C - \Phi_c - h(\rho_0)$, so that:

$$F(f_0) = h^{-1}\left[C - C + \Phi_c + h(\rho_0) - \Phi_c\right] = h^{-1}\left[h(\rho_0)\right] = \rho_0, \tag{3.23}$$

because h^{-1} is a function inverse to h. We simply get

$$f_1 = \mathcal{R}(\rho). \tag{3.24}$$

Using definition of the canonical function (3.17), $f_1 = C - \Phi_c - h(\rho_1)$, and

$$C - \Phi_c - h(\rho_1) = \mathcal{R}(\rho). \tag{3.25}$$

This is our first order approximation for density distribution ρ_1. For given approximate density distribution ρ_0, we expect, from formula (3.25), to calculate better approximation ρ_1. In a general case of ρ_0, explicit (usually numerical) integration in eq. (3.25) is inevitable. This was motivation of the numerical methods development. But if we are able to calculate numerically first order approximation, it is obvious that we are able to calculate arbitrary number of terms (3.20). Calculating only first term in (3.20) seems to be pointless for such a case, as we are ready to repeat this integration as many times as needed.

3.3.3 *Zeroth-order approximation*

Sometimes we are able to calculate the integral in eq. (3.25), as e.g. for constant density ball or point mass. However, it is also possible to eliminate the integral operator from eq. (3.25) for a wide class of compressible objects. Consider a special case of equation (3.6) for $\Phi_c \equiv 0$ i.e. with no rotation:

$$h(\rho) + \mathcal{R}(\rho) = C. \tag{3.26}$$

When we use a function which satisfies eq. (3.26) as zero-order (ρ_0) approximation

$$h(\rho_0) + \mathcal{R}(\rho_0) = C_0, \tag{3.27}$$

integration in eq. (3.25) can be easily eliminated:

$$C - \Phi_c - h(\rho_1) = \mathcal{R}(\rho_0) = C_0 - h(\rho_0). \tag{3.28}$$

3.3.4 *First order approximation for the enthalpy*

Finally, collecting relevant terms of eq. (3.28) on the right-hand side, our formula takes the form:

$$h(\rho_1) = h(\rho_0) - \Phi_c + C - C_0. \tag{3.29}$$

Formula (3.29) reveals importance of enthalpy. Clearly, enthalpy (2.24) is the most relevant physical quantity for description of a rotating body structure. This is not surprise, as e.g.

Eriguchi & Müller [7] have found increase of convergence rate for their computational method if, instead of density ρ, quantity $X = \rho^{\gamma-1}$ is used. For polytropic EOS (3.61), quantity X is proportional to enthalpy (3.63). Actually, rate of convergence for series (3.20) is fast enough to get sensible results from the first-order approximation (3.25). Enthalpy is thus more convenient physical quantity than density, and we may write

$$h_1 = h_0 - \Phi_c + C - C_0. \tag{3.30}$$

We have got very simple expression (3.30). Functions denoted by subscript '0' are simply distributions of physical quantities of non-rotating barotropic stars. In case of polytropic EOS (3.61) density and enthalpy are given by Lane-Emden functions.* In case of general barotropic EOS (2.1) we have to find zeroth-order distribution by means of solving ordinary differential equation of hydrostatic equilibrium (2.22). Centrifugal potential Φ_c, defined in (2.39), is known, according to our assumption of permanent rotation (2.30) and Poincaré-Wavre theorem (p. 19).

3.4 Properties of the approximate formula

According to eq. (3.27) the constant C_0 is directly related to zeroth order density ρ_0. For given ρ_0 we are able to determine C_0, and *vice versa*. Therefore, we should write our formula as:

$$h_1 = h_0(C_0) - \Phi_c + C - C_0, \tag{3.31}$$

where we indicated explicitly one-to-one relation between C_0 and h_0. Eq. (3.31) has the two free parameters: C and C_0. As we have already pointed out, the constant C in eq. (3.6) labels the family of solutions with different total mass, but the same physical conditions i.e. EOS and rotation law. Simply speaking, C defines the size of a star we are looking for. Constant C_0 and the associated function $\rho_0(C_0)$ should be adjusted to find approximation h_1 as close to solution of eq. (3.6) as possible. To do this we have to define mathematical criteria of the approximation accuracy. We will use virial test (3.47), which is a popular astrophysical tool for testing numerical schemes [24].

3.4.1 *Re-arrangement of the formula*

Manipulating both ρ_0 and C_0 is very inconvenient. Instead of this we may try to find equation (actually defined by C) for which h_0 is best zero-order approximation. This is, of course, equivalent problem. Zero-order approximation $\rho_0(C_0)$ is then fixed now. We define new constant value:

$$\Delta C = C_0 - C, \tag{3.32}$$

and our first-order formula becomes

$$h_1 = h_0 - \Phi_c - \Delta C. \tag{3.33}$$

Now, h_0 is a fixed function. Advantage of the eq. (3.33) over eq. (3.30) is clear: now we have to manipulate single real number ΔC instead of manipulating both C_0 and function h_0.

3.4.2 *Structure of the formula*

Fig. 3.3 presents schematic graphs of first two terms in eq. (3.33), explaining the meaning of ΔC. Actually, an enthalpy distribution is function of two variables: $h = h(r, z)$. Rotation

*Cf. APPENDIX B on page 58.

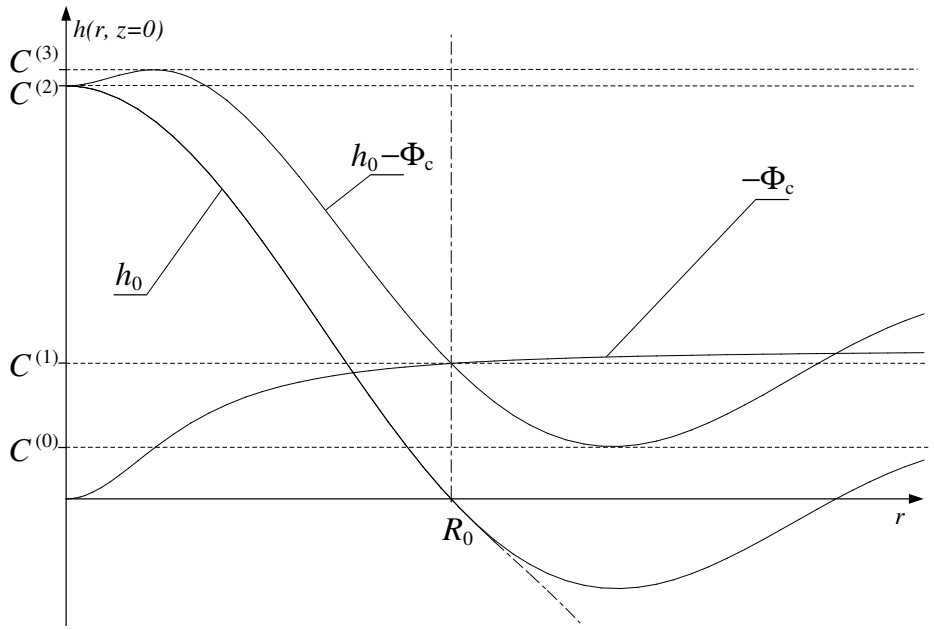

Figure 3.3: Overview of various terms in the formula (3.33).

however, acts most strongly along the equatorial plane $z = 0$, therefore equatorial plane has been chosen to overview of our formula in Fig. 3.3. Important values of ΔC are denoted as $C^{(i)}$. The most general case is shown in Fig. 3.3. In particular cases some of constants C may not exist: $C^{(0)}$ – if h_0 monotonically decreases to $-\infty$ and $C^{(2)}$ – if h_0 decreases faster than Φ_c grows. This depends on the both h_0 and Φ_c. Vertical dot-dashed line in Fig. 3.3 indicates that $C^{(1)} = \Phi_c(R_0)$, where R_0 is the radius of non-rotating star. The dashed curve fragment below the axis reflects ambiguity of the Lane-Emden function continuation to negative values.

The role of constant ΔC is clear from Fig. 3.3: it defines a cutoff value for sum of two positive functions h_0 and $-\Phi_c$. We have chosen $n = 1$ Lane-Emden function $\sin r/r$ to prepare Fig. 3.3. In this case* Lane-Emden function behaviour is oscillatory, and the centrifugal potential may be strong enough to rise the entire function $h_0 - \Phi_c$ above $h = 0$ plane, cf. Fig. 3.3. This extremal case makes importance of ΔC obvious: using a tempting value of $\Delta C = 0$ we get infinite equatorial radius. This example shows, that value of ΔC has to be determined carefully. Nevertheless, it is not a trivial task.

3.4.3 *Physical interpretation of the formula*

Structure of our formula reflects our physical intuition as to the behaviour of the rotating objects as follow:

I. Non rotating object is described by spherically symmetric distribution of the enthalpy $h_0(r, z)$,

II. Rotation, namely the centrifugal force, moves matter outward, acting against gravity. This is realized by the addition of the (minus) centrifugal potential: $h_0(r, z) - \Phi_c(r)$,

*And any other odd polytropic number n case.

III. But matter flows from central region to outer part of a body, therefore density (thus enthalpy, cf. (3.63)) in the central region has to be decreased – this is realized by subtraction of the constant value ΔC.

3.4.4 *Values of constants in the formula*

Essential part of the formula (3.30) are constants C and C_0. Determination of constant $\Delta C = C - C_0$ is crucial, and decides whether our formula becomes accurate or fails completely.

Question thus arises what value for ΔC should be chosen. First, we try get overview of the ΔC general properties.

I. If the value of ΔC is chosen too low or negative, equatorial radius of the enthalpy approximation may become infinite. This case, however, is not possible if zeroth-order enthalpy monotonically decreases to minus infinity, as e.g. for Lane-Emden functions with even polytropic index n. In other words, limiting value of ΔC, denoted as $C^{(0)}$ in Fig. 3.3 equal to minimum value $C^{(0)} = min(h_0 - \Phi_c)$, may not exist, as a function $h_0 - \Phi_c$ may not possess minimum. The value of ΔC should be chosen, of course, to be greater than $C^{(0)}$. If $C^{(0)}$ does not exist, in principle any value from $-\infty$ could be considered.

II. The value of $\Delta C = -\Phi_c(R_0)$, denoted as $C^{(1)}$ in Fig. 3.3, seems to be of great importance, because it divides enthalpy distributions into two classes. If $\Delta C < C^{(1)}$, we shift function $h_0 - \Phi_c$ down, but not enough to avoid negative values of zeroth-order approximation. Negative values are unphysical, so intuitively we would like to reject those values of ΔC. Moreover, in many interesting cases, continuation of Lane-Emden function beyond first zero-point with negative values leads to complex values. Detailed examination of the formula accuracy have shown failure of this idea – negative values of h_0 are required to get accurate results.

III. Another interesting value of ΔC is the central enthalpy $h_0(r = 0, z = 0)$ of non-rotating configuration, denoted in Fig. 3.3 as $C^{(2)}$. If we put ΔC slightly above $C^{(2)}$, in our approximation for enthalpy distribution a central hole appear. Such toroidal configurations are then possible to obtain within framework of our approximation, but they are far beyond applicability of our formula. Moreover, such configurations are likely to be unstable, thus out of physical importance.

IV. For values above maximum $\Delta C = max(h_0 - \Phi_c)$ the enthalpy is identically zero. Actually, from (3.33) h_1 is negative, but we are cutting off negative values in final result.

3.4.5 *Summary of the approximation procedure*

Let us summarize procedure leading to approximate enthalpy distribution for differentially rotating bodies:

1. We choose non-rotating, spherically symmetric initial enthalpy distribution h_0.

2. We prescribe rotation law $\Omega = \Omega(r)$, and calculate centrifugal potential according to definition (2.39).
3. We choose ΔC and calculate h_1 from (3.33)
4. Any negative part of enthalpy calculated that way is cut off.
5. Remaining positive function is our approximate enthalpy distribution of the rotating body.

3.5 Analytical solutions for ΔC

The procedure steps 1-5 formulated in the previous subsection require knowledge of the ΔC. We discuss the proposed methods in this section.

3.5.1 *The simplest method for* ΔC

Our first proposition for constant in eq. (3.33) is:

$$\Delta C = -\Phi_c(R_0). \tag{3.34}$$

The value of ΔC ($C^{(1)}$ in Fig. 3.3) defined above may be used as a first step towards more accurate value. It is very simple to calculate, and in many interesting cases can be computed analytically. Therefore, our formula takes the form:

$$h_1 = h_0 - \Phi_c + \Phi_c(R_0), \tag{3.35}$$

where all quantities are usually known. Unfortunately, global properties of rotating body (cf. Table 3.1, Fig. 3.8, 3.9) are poorly predicted. Nevertheless, the shape of the iso-enthalpy contours in the central region is almost unaffected by small changes of ΔC. Formula (3.35) is then excellent tool for those who are interested in quantitative outlook of the rotating body internal structure.

3.5.2 *Averaged centrifugal potential*

We may also try to substitute our formula (3.33) into basic equation (2.42):

$$h_0 - \Phi_c + \Delta C + \Phi_g(h_1) + \Phi_c = C, \tag{3.36}$$

and using eq. (3.32) we get:

$$h_0 + \Phi_g(h_1) - C_0 = 0, \tag{3.37}$$

but, according to eq. (3.27), $h_0 - C_0 = -\mathcal{R}(\rho_0) \equiv \Phi_g(h_0)$ and thus

$$\Phi_g(h_0) = \Phi_g(h_1). \tag{3.38}$$

This equality is true only if

$$h_0 = h_1, \tag{3.39}$$

where h_1 is calculated from eq. (3.33), and we obtain:

$$-\Phi_c = \Delta C. \tag{3.40}$$

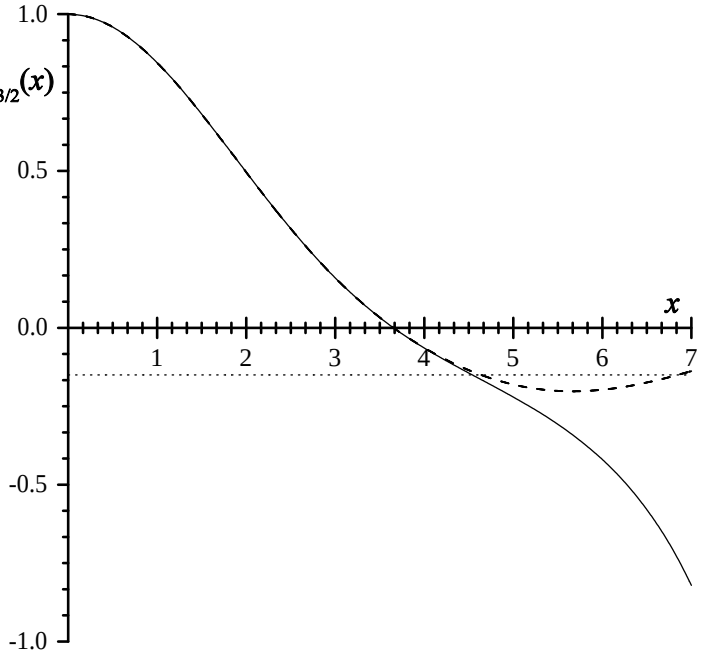

Figure 3.4: In general, continuation of Lane-Emden functions to negative values leads to the complex numbers. Therefore, we have to modify original Lane-Emden equation. Unfortunately, such a modification cannot be done unambiguously. Two possible modifications (as described in text) lead to functions marked by solid and dashed lines, respectively. Fortunately, these two solutions do not differ significantly for values slightly below zero. As it is marked by dotted horizontal line, if $w > -0.15$, differences between these two functions are almost negligible.

In eq. (3.40) above, the left-hand side is a function, while the right-hand side is constant. Equality (3.40) is then fulfilled only in trivial case $\Delta C \equiv \Phi_c \equiv 0$. To handle this problem, we propose to average the centrifugal potential,

$$\widehat{\Phi_c} = (V_0)^{-1} \int\limits_{V_0} \Phi_c \, d^3\mathbf{r}, \tag{3.41}$$

over the volume V_0 of a non-rotating initial configuration. Using the averaged value of $\Phi_c(r)$, we are able to calculate ΔC:

$$\Delta C = -\widehat{\Phi_c}. \tag{3.42}$$

A method used to calculate the average value of Φ_c (3.42) is in principle free to choose. Eq. (3.41) is just the simplest possibility.

Remarkable property of ΔC given by the average value of centrifugal potential (3.41) is that (3.42) is always below $-\Phi_c(R_0)$ i.e. $C^{(1)}$ from Fig. 3.3. We can see this as follow. The mean value theorem states that any average value is always between minimum and maximum value in a given area. Centrifugal potential is a monotonic function with a maximum at $r = 0$ and a minimum* at $r = R_0$. Therefore any average over volume of $R = R_0$ ball satisfies inequality:

$$\Delta C = -\widehat{\Phi_c} < -\Phi_c(R_0) = C^{(1)} \tag{3.43}$$

This statement does not depend on the averaging method. In this case continuation of initial function h_0 to negative values is required for successful approximation. This important result is confirmed by numerical calculations using virial test.

3.5.3 *Continuation of the zeroth-order initial approximation h_0 to negative values*

We continue discussion of the behaviour of functions describing structure of non-rotating barotropes beyond the first zero-point. From physical argument we are unable to tell how to extend such

*Function $-\Phi_c$ is non-negative. We consider extrema of Φ_c over volume of ball with a radius R_0.

functions, because quantities like pressure and density are always non-negative.

From mathematical point of view, there is no reason to avoid negative values, and we do not expect any difficulties. Unfortunately, physically interesting cases, like non-relativistic degenerate electron gas EOS, leads to equations with fractional power terms. Such equations are subject to continuation with complex values. This is extremely bad behaviour, as these values are used to predict physical quantities like enthalpy, density, pressure etc. Simple, but successful modification of the basic equation is, however, possible to avoid these problems.

We concentrate on a polytropic EOS. Physical quantities for polytropes are expressed in terms of Lane-Emden functions (cf. APPENDIX B). As we have pointed out, for the original Lane-Emden equation

$$\frac{d^2w}{dx^2} + \frac{2}{x}\frac{dw}{dx} + w^n = 0, \tag{3.44}$$

solution $w(x)$ has no real negative values if n is a fraction, e.g. $n = 3/2$. We can easily modify last term of eq. (3.44) to get required behaviour of the solution. If we substitute:

$$\ldots + w^n \rightarrow \ldots + |w|^n, \tag{3.45}$$

or:

$$\ldots + w^n \rightarrow \ldots + \mathrm{sign}(w)|w|^n, \tag{3.46}$$

then for $w(x) > 0$ we get the same solution as for (3.44). For both substitutions, (3.45) and (3.46) we get real values beyond the first zero-point of $w(x)$. Nevertheless, no hint exists to help us to choose between (3.45) and (3.46). From practical point of view, we found very small difference (cf. Fig. 3.4) between solutions of Lane-Emden equation modified according to (3.45) and (3.46), respectively, if $w(x) << 1$. In contrast to global quantities, the surface region of our approximation may be significantly affected by theses differences. This, at least partially, explains a poor approximation to axis ratio (cf. Fig. 3.10, 3.11) of the rotating configuration.

Modification (3.45) leads to solutions of eq. (3.44) similar to those for even (integer) n, while (3.46) leads to odd-like behaviour. In our calculations we will consequently use the modification (3.45).

3.6 Numerical determination of $\triangle C$

3.6.1 *Virial theorem*

Scalar virial theorem for rotating stars states that:

$$2\,E_k - |E_g| + 3\iiint_V p(\mathbf{r})\,d^3\mathbf{r} = 0, \tag{3.47}$$

where E_k is rotational kinetic energy:

$$E_k = \frac{1}{2}\iiint_V \rho(\mathbf{r})\,(\Omega\,r)^2\,d^3\mathbf{r}, \tag{3.48}$$

and r denotes distance from rotation axis. E_g is gravitational energy:

$$E_g = -\frac{1}{2}\,G\int_{V\times V}\cdots\int \frac{\rho(\mathbf{r})\rho(\mathbf{r}')}{|\mathbf{r}-\mathbf{r}'|}\,d^3\mathbf{r}\,d^3\mathbf{r}'. \tag{3.49}$$

Remaining term is the volume integral of pressure p. All integrals in (3.47) are over the entire volume V of a star. Derivation of the virial equations in general case can be found in e.g. [3].

3.6.2 *Virial test of the formula*

Using virial theorem we are able to find the best possible value of ΔC. If for some value of ΔC the virial test is satisfied, we suppose that for this value we get the best approximation.

Let us define the virial test parameter Z:

$$Z = \frac{2E_k - |E_g| + 3\int p d^3\mathbf{r}}{|E_g|}. \tag{3.50}$$

This parameter reflects departure from the global equilibrium. For any structure in equilibrium, the virial test parameter is equal to zero.

We demand, the constant ΔC to satisfy:

$$Z(h_0 - \Phi_c - \Delta C) = 0. \tag{3.51}$$

3.6.3 *Other methods*

Although the virial test seems to be a natural method for determination how close the global equilibrium is approached, we may also use other criteria.

Direct comparison of rotating star structure given by numerical procedure, $h_{num}(r, z)$, and our approximate formula $h_1(r, z)$ should be made using e.g. the least squares method. Therefore, our free parameter ΔC could be determined from the requirement:

$$\int [\ h_0 - \Phi_c - \Delta C - h_{num}\ ]\, d^3\mathbf{r} = min. \tag{3.52}$$

If successful, such a method would provide us with simple fitting formulae for numerical results.

3.7 Widely used angular velocity profiles

At present, we are unable to derive angular velocity profile inside rotating stars from basic principles, e.g. from stellar evolution. It is not even known, whether strongly differentially rotating objects are present in the Universe. Therefore, we are almost free in making decision what is rotation law inside our object.

Nevertheless, most of possible rotating laws can be immediately excluded on basis of the stability analysis (cf. APPENDIX D). Examples of angular velocity profiles presented in the following subsections obey basic stability criteria.

3.7.1 Rigid rotation

Rigid (aka uniform, homogeneous) rotation is a motion with the constant angular velocity $\Omega(r) = \Omega_0$. This is the most carefully studied example and numerous successful methods exist there. This is fortunate for us, because our method seems to fail if rotation is uniform. Some astrophysicists state, that only homogeneous rotation is allowed, due to internal stress forces. These forces (viscosity, magnetic fields) force rotation to be rigid. Our knowledge of such forces in usually very exotic stellar interiors is unfortunately poor. Therefore, we cannot

exclude differential rotation* in stellar interiors. It is more than probable, that strong differentiability exists in massive stars at late stages of evolution [13, 14]. Recent results show, however, that rotation strength and differentiability may be smaller than previously calculated [15].

If $\Omega = const$, the centrifugal potential is very simple:

$$\Phi_c = -\frac{1}{2}{\Omega_0}^2\, r^2. \tag{3.53}$$

Let us note, that for rigid rotation $\Phi_c \xrightarrow{r\to\infty} -\infty$, in contrast to differential rotation, where usually $\Phi_c \xrightarrow{r\to\infty} const$**. This, at least partially, explains why centrally condensed bodies are unable to store large amount of angular momentum. These objects, are usually of a big radius, therefore Φ_c fast reaches huge values. Our approximation (3.33) shows direct relation between Φ_c and distortion of a star. Accordingly, in case of rigidly rotating centrally condensed body it is impossible to maintain sensible deformation even if Ω_0 is small. In contrast, for differential rotation, Φ_c may be small for a big radius, even in case of enormous angular velocity at the rotation axis.

3.7.2 *The j-const rotation law*

In our thesis we have used so-called j-const and v-const rotation laws of Eriguchi & Muller [7]. Both of them are stable, cf. APPENDIX D.

The j-const (j – angular momentum) angular velocity profile is defined by:

$$\Omega(r) = \frac{\Omega_0}{1 + (r/A)^2}. \tag{3.54}$$

According to (2.39), centrifugal potential is:

$$\Phi_c(r) = -\frac{1}{2}\frac{\Omega_0^2\, r^2}{1 + (r/A)^2}. \tag{3.55}$$

The name j-const reflects the behaviour of (3.54) for $A \to 0$:

$$\Omega(r) = \frac{A^2\Omega_0}{A^2 + r^2} \sim \frac{A^2\Omega_0}{r^2}. \tag{3.56}$$

Specific angular momentum is defined as $j = \rho\,\Omega(r)\,r^2$. Therefore $\Omega(r)$ behaves as for rotating body with $j = const$.

If $A \to \infty$ then $\Omega(r) \to \Omega_0$ i.e. it corresponds to the uniform rotation.

3.7.3 *The v-const rotation law*

The v-const (v – velocity) rotation law is defined by:

$$\Omega(r) = \frac{\Omega_0}{1 + r/A}. \tag{3.57}$$

*Our discussion is for strong differentiability and high rotation rate, where the mechanical equilibrium is significantly affected by the centrifugal forces. Some sort of the differential rotation has to be present in the stars, to drive the magnetic field generation via dynamo mechanism. Usually, rotation required by the stellar dynamo is not strong enough to distort a star. Nevertheless, close connection of differential rotation and magnetic fields beyond any doubt. At present we may only guess processes driving magnetic fields in such objects as magnetars.

**This is generally not true, because $\Omega(r)$ may exhibit $const$-like behaviour. Nevertheless, widely used rotation laws (3.54, 3.57) satisfy this condition.

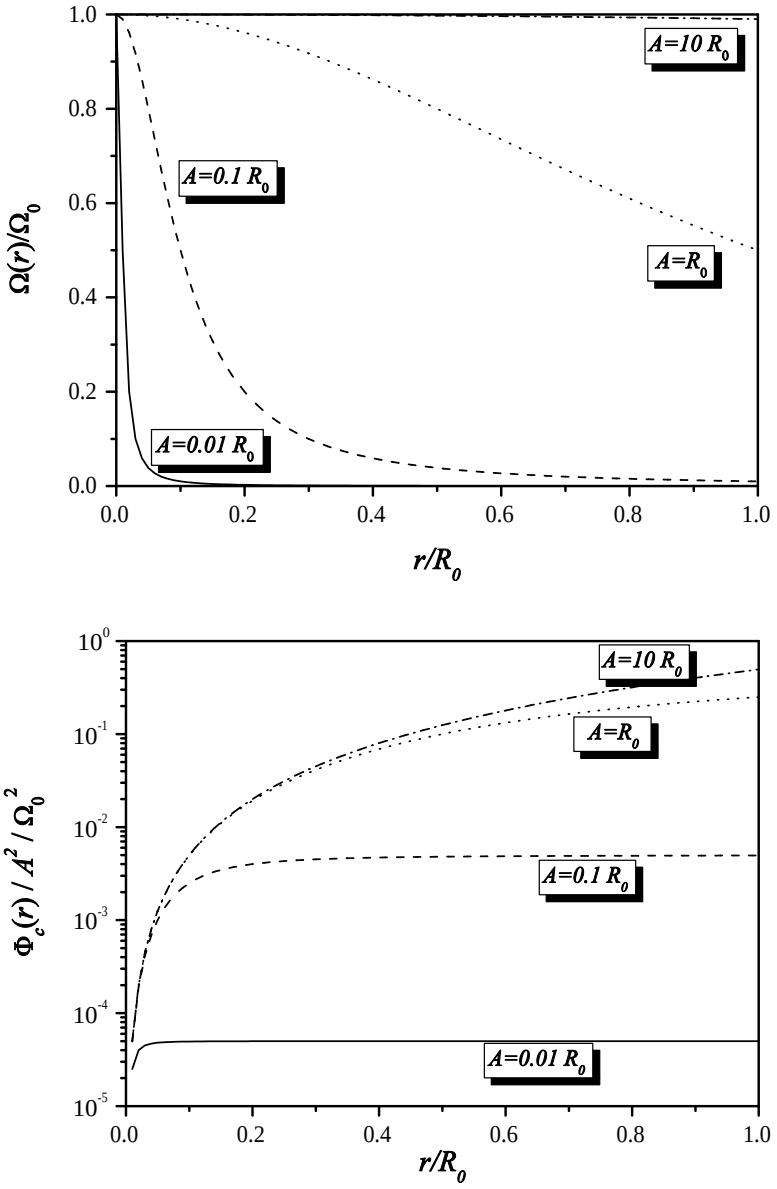

Figure 3.5: Angular velocity profiles (upper) and resulting centrifugal potentials (lower) in case of j-const rotation law (3.54, 3.56). Horizontal axis is scaled in units of equatorial radius R_{eq}. Four cases of differentiability are shown: $A = 0.01R_0$ (solid), $A = 0.1R_0$ (dashed), $A = R_0$ (dotted) and $A = 10R_0$ (dash-dotted). For extremal differentiability (solid) angular momentum is concentrated at the rotation axis, and the centrifugal potential is constant over outer parts of a body. In contrast, almost uniform rotation (dash-dotted, dotted), leads to monotonically increasing centrifugal potential.

According to (2.39), centrifugal potential is:

$$\Phi_c(r) = -\Omega_0^2 A^2 \left[\frac{1}{1 + A/r} - \ln(1 + r/A) \right]. \tag{3.58}$$

Similarly to the case described in the previous subsection, the name v-const reflects the behaviour of (3.57) for $A \to 0$:

$$\Omega(r) = \frac{A\Omega_0}{A + r} \sim \frac{\Omega_0}{r}. \tag{3.59}$$

Accordingly, because of the relation $v = \Omega(r)\, r$ between angular and linear velocity, $\Omega(r)$ behaves as for matter rotating with constant linear velocity v.

Again, if $A \to \infty$ then $\Omega(r) \to \Omega_0 = const$.

3.7.4 *Stoeckley's angular velocity*

In numerical calculations [27], the following differential angular velocity profile has been used:

$$\Omega(r) = \Omega_c \, \exp\left(-a \, \frac{r^2}{R_e} \right), \tag{3.60}$$

where R_e is the equatorial radius. The Solberg criterion requires, for stability reasons, $0 \leq a \leq 1$. As we can see from this example, if angular velocity is decreasing too fast with the radius (e.g. exponentially), we can easily violate the Solberg-Høiland criterion of stability.

3.8 Testing our formula

3.8.1 *The polytropic EOS*

The most popular example of barotropic equation of state (2.1) is the polytropic EOS defined as:

$$p(\rho) = K \, \rho^{\gamma}, \tag{3.61}$$

where γ is referred to as the polytropic exponent. Polytropic index n is defined by the equation:

$$\gamma = 1 + \frac{1}{n}. \tag{3.62}$$

The most relevant properties of non-rotating polytropes are summarized in APPENDIX B.

We will use the structure of differentially rotating polytropes computed in [7] as reference data to test quality of our approximate formula (3.33).

3.8.2 *Rotating polytropes*

In case of polytropic EOS (3.61) the enthalpy is:

$$h(\rho) = \frac{K\gamma}{\gamma - 1} \rho^{\gamma - 1}. \tag{3.63}$$

Zeroth-order approximation of density (the density of non-rotating polytrope, see: [17], APPENDIX B) with n-th Lane-Emden function w_n is:

$$\rho_0 = \rho_c \left[w_n(Ar) \right]^n, \qquad A^2 = \frac{4\pi G}{nK\gamma} \rho_c^{\frac{n-1}{n}}. \tag{3.64}$$

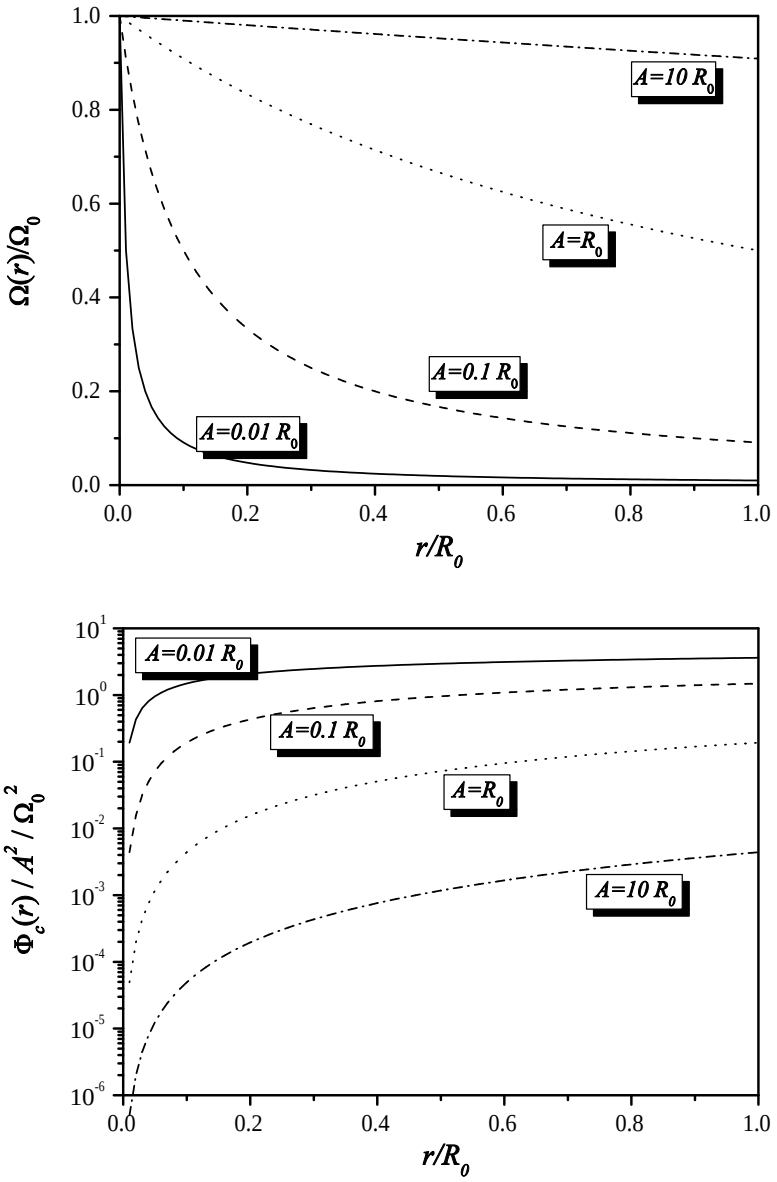

Figure 3.6: Angular velocity profiles (upper) and resulting centrifugal potentials (lower) in case of v-const rotation law (3.57, 3.58). Axes units and description the same as in Fig. 3.5. Four cases of differentiability are shown.

and our formula for density becomes:

$$\rho_1 = \left[{\rho_c}^{1/n} w_n - \frac{1}{nK\gamma}(\Phi_c + \Delta C), \right]^n , \tag{3.65}$$

where ΔC is calculated from (3.40), (3.34) or (3.51).

Now we concentrate on $n = 3/2$ polytrope. In our calculations and figures we will use $4\pi G = 1$, $\rho_c = 1$ and $K = 2/5$. Now the formula (3.65) becomes:

$$\rho_1 = (w_n - \Phi_c - \Delta C)^{3/2} . \tag{3.66}$$

3.8.3 *Global properties of rotating polytrope*

To test the accuracy of our approximation we have calculated the axis ratio, total energy, kinetic to gravitational energy ratio, and dimensionless angular momentum. The axis ratio is defined as usual as:

$$\varepsilon = \frac{R_z}{R_{eq}}, \tag{3.67}$$

where R_z is distance from the centre to the pole and R_{eq} is the equatorial radius. The total energy E_{tot}:

$$E_{tot} = (E_k + E_g + U)/E_0 \tag{3.68}$$

is normalized by:

$$E_0 = (4\pi G)^2 \frac{M^5}{J^2}, \tag{3.69}$$

and the dimensionless angular momentum is defined as:

$$j^2 = \frac{1}{4\pi G} \frac{J^2}{M^{10/3}} \rho_{max}^{1/3}, \tag{3.70}$$

where M and J are the total mass and angular momentum, respectively; ρ_{max} is the maximum density. Quantities (3.67)-(3.70) are computed numerically (cf. APPENDIX C) from (3.66), with given angular velocity $\Omega(r)$ and chosen ΔC. We measure strength of rotation using rotational to gravitational energy* ratio:

$$\beta = \frac{E_k}{|E_g|} \tag{3.71}$$

3.8.4 *Properties of* ΔC

Figure 3.7 show results of the three methods proposed for proper evaluation of ΔC. As we will show in the next subsections, the formula (3.33) can be significantly improved by using virial test (3.47) to determine ΔC. In contrast to results obtained from simple analytical values (3.34, 3.40), ΔC from eq. (3.51) requires iterative numerical solution of the equation involving multiple integrals for gravitational energy, kinetic energy etc. This virtually cancels the convenience given by simplicity of our formula.

Fortunately, a closer look at $\log - \log$ plot (Fig. 3.7) of functions $\Delta C(\Omega_0)$ reveals the fact that they are just straight lines. This strongly suggest, that power law

$$\Delta C = a \ (\Omega_0)^\alpha \tag{3.72}$$

*To avoid misunderstands, we note that both E_k and E_g are calculated for the rotating body, not initial spherically symmetric configuration.

Ω_0	ε	j^2	β	$-E_{tot}/E_0$	Virial test Z	$\widetilde{Z}$	ΔC	$\Delta\widetilde{C}$
0.25	1.01	8.41×10^{-5}	0.004	2.50×10^{-6}	0.01	0.01	0.01	0.01
0.50	1.05	3.38×10^{-4}	0.02	1.00×10^{-5}	0.03	0.04	0.03	0.03
0.75	1.15	7.64×10^{-4}	0.04	2.20×10^{-5}	0.07	0.10	0.07	0.08
1.00	1.19	1.37×10^{-3}	0.07	3.80×10^{-5}	0.12	0.17	0.12	0.14
1.25	1.31	2.17×10^{-3}	0.10	5.56×10^{-5}	0.19	0.28	0.19	0.21
1.50	1.46	3.12×10^{-3}	0.15	7.38×10^{-5}	0.27	0.43	0.27	0.31
1.75	1.68	4.40×10^{-3}	0.20	8.93×10^{-5}	0.36	0.63	0.37	0.42
2.00	1.98	5.90×10^{-3}	0.26	9.89×10^{-5}	0.47	0.89	0.48	0.55
2.25	2.45	7.55×10^{-3}	0.32	1.01×10^{-4}	0.57	1.22	0.60	0.69
2.50	3.30	9.30×10^{-3}	0.38	0.94×10^{-4}	0.67	1.66	0.75	0.86
2.75	5.80	1.10×10^{-2}	0.44	0.84×10^{-4}	0.75	2.22	0.90	1.04

Table 3.1: Properties of $n = 3/2$ polytropic model (3.66) with j-const rotation law and $A = 0.2R_0$. ΔC is calculated from eq. (3.40) and $\Delta\widetilde{C}$ from eq. (3.34). The virial test parameter in the latter case is labeled by $\widetilde{Z}$. By little change from $\Delta\widetilde{C}$ to ΔC one can notice significant improvement of the virial test. In both cases the virial test suggest strong deviation from equilibrium, especially for strong rotation. Actually, the virial test parameter is a function of the ΔC. We can require the virial theorem to be satisfied, by use of another value for ΔC, the solution of eq. (3.51). The results can be improved significantly in this way – compare with Table 3.2 and Fig. 3.9.

can be used to re-derive results of (3.34), (3.40) and (3.51). This is not interesting in case of analytical formulae (3.34, 3.40), as $\Delta C \sim \Omega_0^2$ naturally appears there. Indeed, fitting power law gives $\alpha = 2.00$ in both cases, as we expected.

Completely non-trivial, however, is the virial test. We are able to calculate ΔC from the power law with $\alpha = 2.18$. For example, values presented as a dotted line in Fig. 3.7 can be calculated simply with use of eq. (3.72) with $a = 0.08$ and $\alpha = 2.18$. This greatly simplifies calculating ΔC, and allow us to use the formula in analytical form satisfying the virial test automatically.

Nevertheless, it should be carefully studied if exponent $\alpha \simeq 2.2$ has the universal character or depends on e.g. polytropic index, rotation law etc.

3.8.5 *Improvement of the formula by the proper choice of* ΔC

We have made a comparison of our $n = 3/2$ model (3.66) with j-const rotation law and $A = 0.2R_0$ for different values of ΔC with the results of Ref. [7] (Table 1b). Table 3.1 shows our results for ΔC from eq. (3.40). The value of $\Delta\widetilde{C}$ from eq. (3.34) and the corresponding virial test parameter $\widetilde{Z}$ is included here for comparison. Table 3.2 shows global properties of our approximation with ΔC equal to the solution of eq. (3.51), i.e. satisfying the virial theorem.

A direct comparison of values from Tables 3.1 and 3.2 to those in Table 1b of [7] may be difficult, because our driving parameter is central angular velocity Ω_0, while in [7], following successful approach of [11], the axis ratio (3.67) is used. More convenient in this case is comparison of figures prepared from data found in Table 1b of [7] and our tables. This is especially

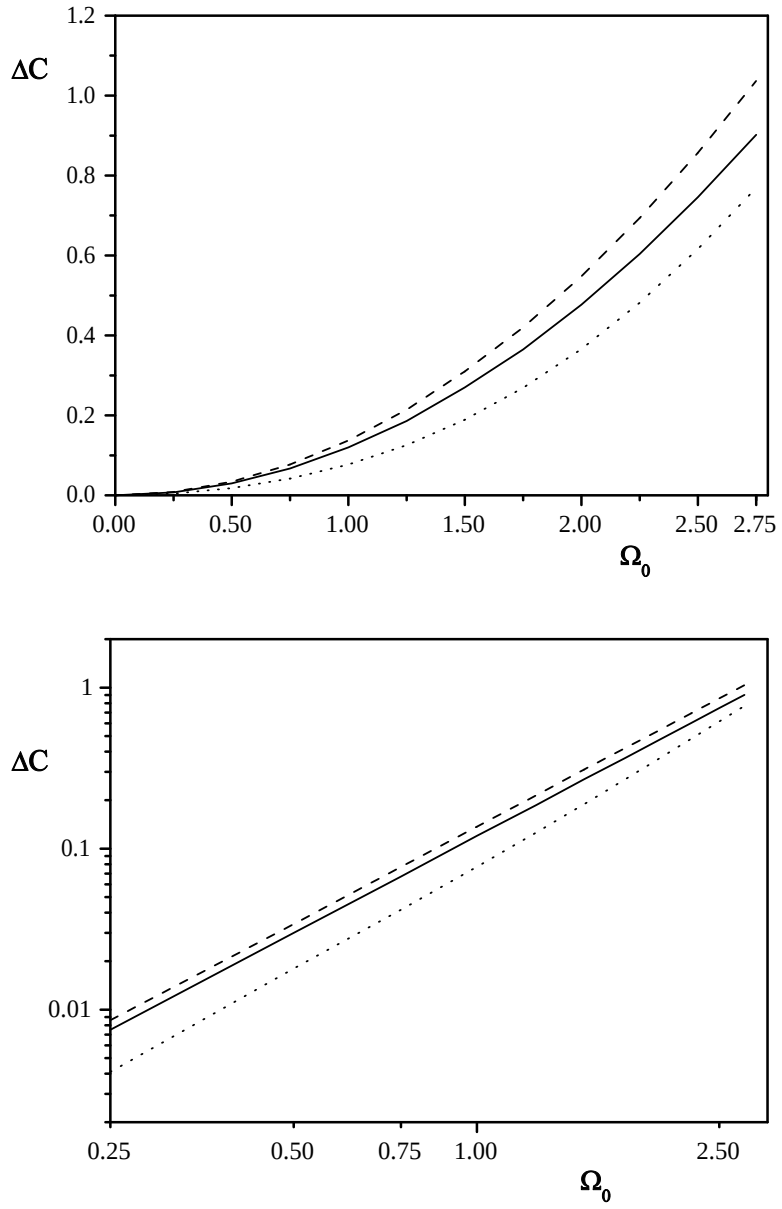

Figure 3.7: Dependence of ΔC on Ω_0, given by eq. (3.34) (dashed), calculated from (3.40) (solid) and given by virial theorem constrain (3.51) (dotted). Both values estimated by (3.40, 3.51) are below $\Delta C = -\Phi_c(R_0)$ i.e. $C^{(1)}$ from Fig. 3.3. It shows, that continuation of Lane-Emden equation to negative values is required for successful approximation of the rotating body structure. From the lower panel ($\log - \log$ plot), we can see that all three choices of ΔC are represented by straight lines, so they are power functions of Ω_0. Density distribution was given by eq. (3.66) with j-const angular velocity with $A = 0.2R_0$.

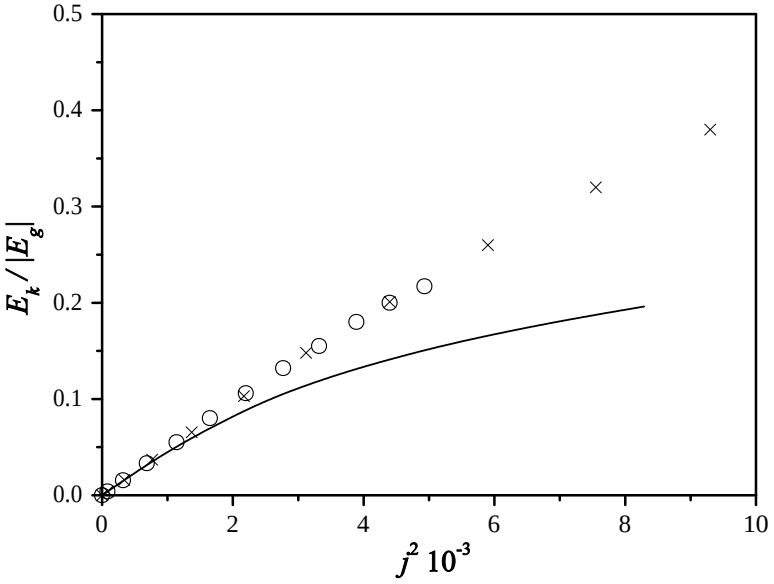

Figure 3.8: $E_k/|E_g|$ ratio as a function of the square of dimensionless angular momentum j^2 for our model (3.66) with $n = 3/2$, $\Omega_0 = 1.5$ and $A = 0.2R_0$. Solid line represents numerical results of [7]. We see that our formula prediction is in good agreement with numerical results if $\beta \ll 0.1$. Results using ΔC from eq. (3.40) are marked by crosses. Results satisfying virial theorem (ΔC from eq. (3.51)) are represented by circles. As it is apparent from figure above, ΔC has no influence on this relation, and cannot improve accuracy of the formula (3.33).

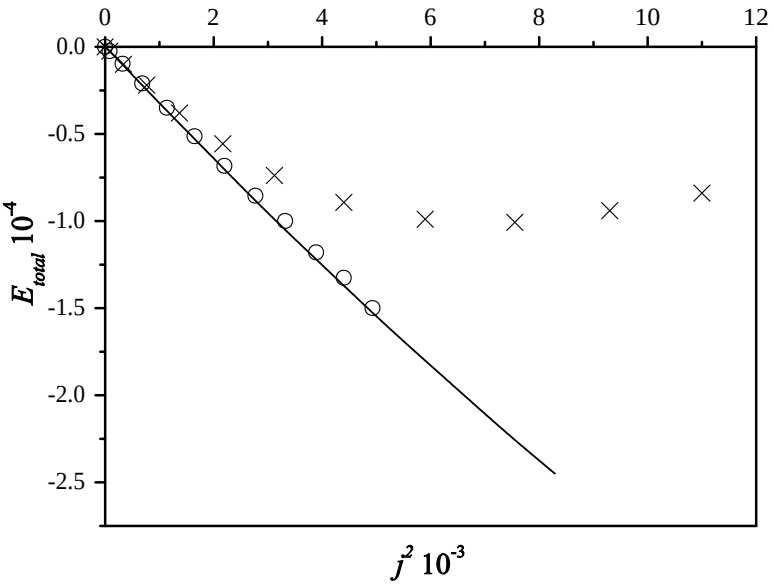

Figure 3.9: Total energy versus j^2. We can see a great improvement of the results with ΔC from eq. (3.51) marked by '$\circ$'. ΔC from eq. (3.40) ($\times$) gives incorrect behaviour of the total energy. Solid line represents results of [7], circles and crosses are result derived from our approximate formula (3.66) with ΔC from virial test (3.51) and eq. (3.40), respectively. The approximation satisfying the virial equation gives results resembling the numerical calculations. The parameters of model are given in the caption of Fig. 3.8.

true, because the axis ratio is not well predicted by our formula (cf. Fig. 3.10 and Fig. 3.11),

Ω_0	ε	j^2	β	$-E_{tot}/E_0$	Virial test $\lvert Z\rvert$	ΔC
0.25	1.01	8.30×10^{-5}	0.004	2.05×10^{-6}	9×10^{-5}	0.004
0.50	1.05	3.22×10^{-4}	0.02	0.98×10^{-5}	3×10^{-4}	0.02
0.75	1.11	6.86×10^{-4}	0.03	2.10×10^{-5}	3×10^{-5}	0.04
1.00	1.20	1.14×10^{-3}	0.06	3.50×10^{-5}	4×10^{-5}	0.08
1.25	1.33	1.65×10^{-3}	0.08	5.14×10^{-5}	6×10^{-4}	0.13
1.50	1.51	2.20×10^{-3}	0.11	6.84×10^{-5}	4×10^{-4}	0.19
1.75	1.74	2.77×10^{-3}	0.13	8.55×10^{-5}	3×10^{-5}	0.27
2.00	2.04	3.32×10^{-3}	0.16	1.00×10^{-4}	1×10^{-3}	0.37
2.25	2.47	3.89×10^{-3}	0.18	1.18×10^{-4}	9×10^{-4}	0.48
2.50	3.12	4.40×10^{-3}	0.20	1.33×10^{-4}	3×10^{-4}	0.62
2.75	4.34	4.93×10^{-2}	0.22	1.50×10^{-4}	1×10^{-6}	0.77

Table 3.2: The same model as in Table 3.1, but now ΔC is derived numerically from eq. (3.51). The virial test parameter shows accuracy of solution to eq. (3.51). Comparison with Table 3.1 and Table 1b of [7] shows significant improvement of the total energy. The axis ratio is also closer to the results of numerical calculations, and the stability indicator β is not unreasonably high. See also Figs 3.8–3.11.

while global properties (E_{tot}, j^2, β, cf. Figs. 3.8, 3.9) and virial test parameter Z are in good agreement if $\beta \ll 0.1$.

Fig. 3.8 shows that our approximation is valid until $\beta \simeq 0.05$, and begins to diverge from numerical results strongly for $\beta \geq 0.1$. Both values of ΔC (3.40,3.51) give similar behavior here. However, ΔC from the virial test produces better results, and β values are more sensible for the strongest rotation.

In contrast, the total energy (3.68) is very sensitive to ΔC. The value of ΔC from eq. (3.40) produces the wrong result. E_{tot} begin to increase for $j^2 \geq 7 \cdot 10^{-3}$, while numerical results give monotonically decreasing E_{tot}. The use of ΔC from (3.51) instead gives correct result, cf. Fig. 3.9.

While the global properties of our model are in good agreement with the numerical results for $\beta \ll 0.1$, the axis ratio tends to be underestimated, even for small values of j^2. Fig. 3.10 and Fig. 3.11 show minor improvements when we use ΔC from the virial test (3.51) instead of the mean value (3.40).

This subsection clearly show how important is the value of constant ΔC. The best results are produced with ΔC from eq. (3.51), therefore this value will be used in the next subsections to investigate the influence of differential rotation parameter A and type of rotation law on our formula accuracy.

3.8.6 *Effects of differential rotation*

In addition to the results from previous subsection (j-const with $A = 0.2R_0$) we have calculated properties of the almost rigidly ($A = 2R_0$) and extremely differentially ($A = 0.02R_0$) rotating model with the same rotation law.

In all three cases we are able to find value of ΔC satisfying eq. (3.51). However, this is not

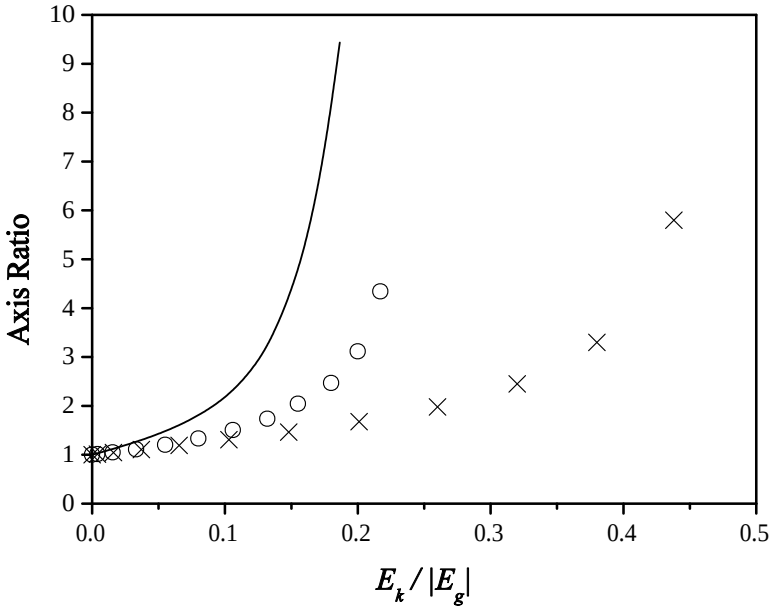

Figure 3.10: Axis ratio versus β. We see that our formula ($\circ, \times$) underestimates the axis ratio. The choice of ΔC satisfying the virial theorem ($\circ$) improves the situation a bit. Solid line again is the result of [7].

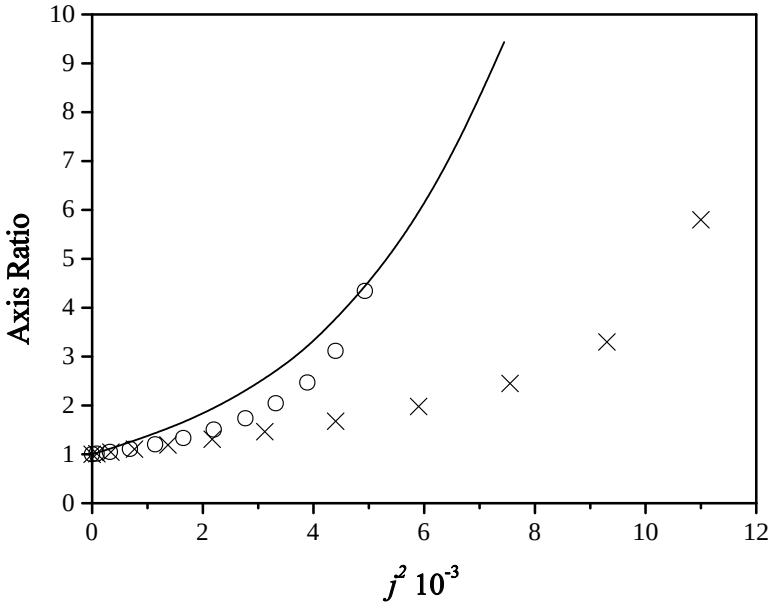

Figure 3.11: Axis ratio vs j^2. The same as in Fig. 3.10. ΔC from eq. (3.50) ($\circ$) gives a better approximation to axis ratio compared to formula (3.40) ($\times$).

enough to find the correct solution, because other parameters describing the rotating body may be wrong. This is clearly shown in Fig. 3.12, where β versus j^2 eq. (3.70) is plotted for three cases of differential rotation. An apparent discrepancy for $A = 2R_0$ exists. Both j-const and v-const angular velocity profiles behave as rigid rotation in this case. Thus we conclude that our formula is unable to predict correct structure in the case of uniform rotation even if the rotation is small.

If the rotation is concentrated near the rotation axis, as in the $A = 0.02R_0$ case, our re-

Ω_0	ε	j^2	β	$-E_{tot}/E_0$	Virial test $\lvert Z\rvert$	ΔC
0.01	1.04	6.10×10^{-6}	1.9×10^{-4}	-1.83×10^{-7}	9×10^{-5}	0.01
0.02	1.20	2.96×10^{-5}	8.7×10^{-4}	-8.80×10^{-7}	1×10^{-4}	0.06
0.03	1.84	1.26×10^{-4}	2.9×10^{-3}	-3.58×10^{-6}	5×10^{-4}	0.15
0.035	2.30	4.49×10^{-4}	7.0×10^{-3}	-1.13×10^{-5}	3×10^{-5}	0.24

Table 3.3: Properties of our approximate sequence in case of j-const rotation law with $A = 2R_0$, i.e. almost uniform rotation. In spite of the fact that the virial test is fulfilled with an accuracy of the order of 10^{-4}, a comparison of the data in this table with the numerical results (cf. Fig. 3.12) clearly shows that our formula fails in the case of rigid rotation.

Ω_0	ε	j^2	β	$-E_{tot}/E_0$	Virial test $\lvert Z\rvert$	ΔC
25	1.01	1.45×10^{-4}	0.02	0.44×10^{-5}	4×10^{-4}	-0.01
50	1.05	4.73×10^{-4}	0.07	1.42×10^{-5}	3×10^{-4}	-0.02
75	1.12	8.31×10^{-4}	0.12	2.47×10^{-5}	4×10^{-4}	-0.03
100	1.23	1.17×10^{-3}	0.16	3.36×10^{-5}	2×10^{-4}	-0.02
150	1.55	1.63×10^{-3}	0.23	4.65×10^{-5}	4×10^{-4}	0.07
200	2.06	1.96×10^{-3}	0.28	5.50×10^{-5}	3×10^{-4}	0.24
250	2.95	2.21×10^{-3}	0.32	6.12×10^{-5}	1×10^{-4}	0.49
300	5.76	2.42×10^{-3}	0.34	6.64×10^{-5}	3×10^{-4}	0.83

Table 3.4: Properties of sequence with j-const rotation law for $A = 0.02R_0$.

sults and the numerical results are of the same order of magnitude. Quantitative agreement is achieved only for very small values of Ω_0. Let us note that in this case ΔC required by virial theorem (3.51) is slightly below zero (Table 3.4). This example shows, that ΔC may also be negative. All three cases are summarized in Fig. 3.12.

The results from this section show, that our formula is able to find the correct structure of the rotating body for differential rotation only. The range of application varies with differential rotation parameters, and the best results are obtained in the middle range i.e. for $A = 0.2R_0$. With the extremal case ($A = 0.02R_0$) the quality of our results is significantly degraded.

In next subsection we examine, if this statement depends on the rotation law.

3.8.7 *Rotation law effects*

In addition to the previously described cases, we have calculated the global properties of our model in the case of the v-const angular velocity profile, with parameters $A = 0.2R_0$ (Table 3.5) and $A = 0.02R_0$ (Table 3.6). The results with $A = 2R_0$ are not presented, because they are similar to the j-const case (cf. Table 3.3), where both functions $\Omega(r)$ behave as for uniform rotation, and our formula fails in this case.

Figures 3.13 and 3.14 show very good agreement of the global physical quantities (β, j^2,

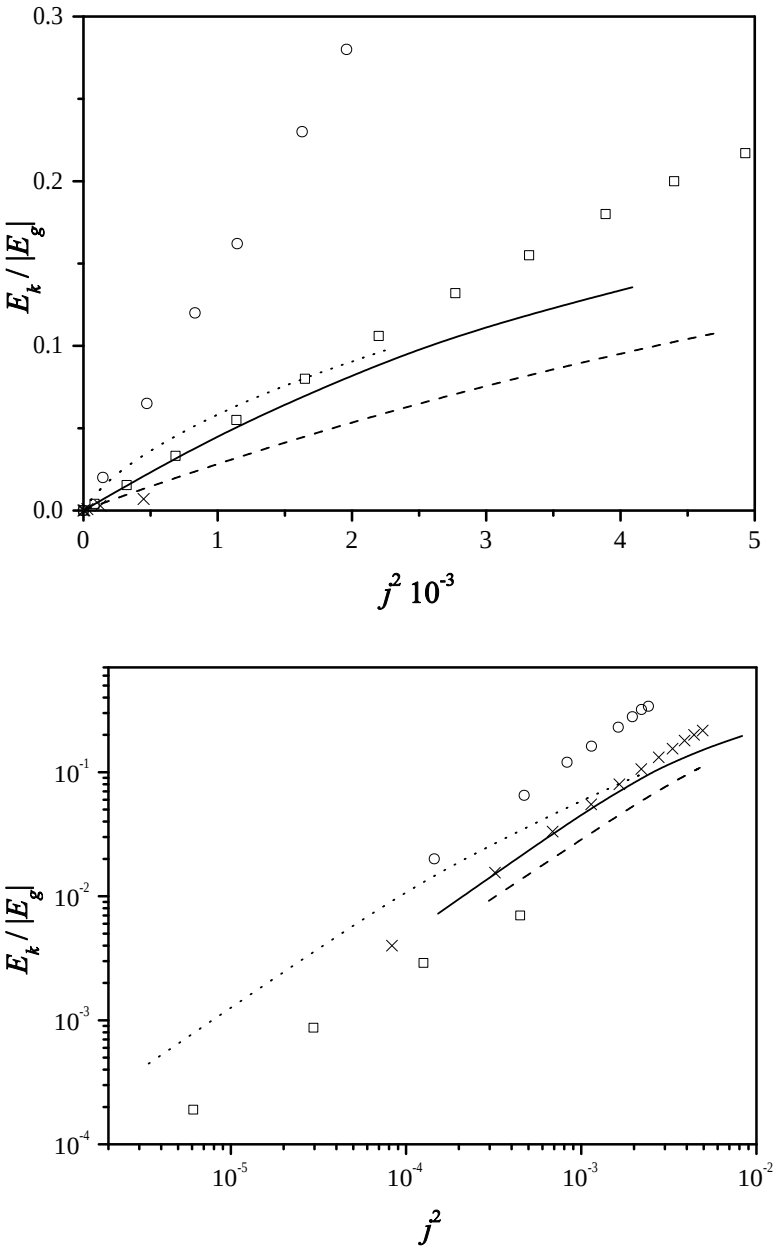

Figure 3.12: Stability indicator β versus j^2 for j-const angular velocity ($\log - \log$ plot) for three values of A. Quantitative agreement between our formula (symbols) and the numerical results ([7], lines) is achieved for $A = 0.2R_0$ if $\beta \leq 0.1$. This case is presented as solid line and crosses. For $A = 0.02R_0$ we have results of the same order, but they are identical only where the rotation strength is very small. This case is presented by dotted line and circles. Our formula fails (dashed line and diamonds) in case of rigid rotation.

Ω_0	ε	j^2	β	$-E_{tot}/E_0$	Virial test $\lvert Z\rvert$	ΔC
0.25	1.05	3.29×10^{-4}	0.01	0.99×10^{-5}	9×10^{-5}	0.01
0.50	1.21	1.41×10^{-3}	0.05	4.26×10^{-5}	2×10^{-4}	0.05
0.75	1.63	3.80×10^{-3}	0.11	1.12×10^{-4}	2×10^{-4}	0.13
1.00	2.31	9.22×10^{-3}	0.21	2.52×10^{-4}	3×10^{-4}	0.27
1.25	5.26	1.44×10^{-2}	0.31	3.87×10^{-4}	5×10^{-4}	0.47

Table 3.5: Properties of our model with v-const rotation law and $A = 0.2R_0$.

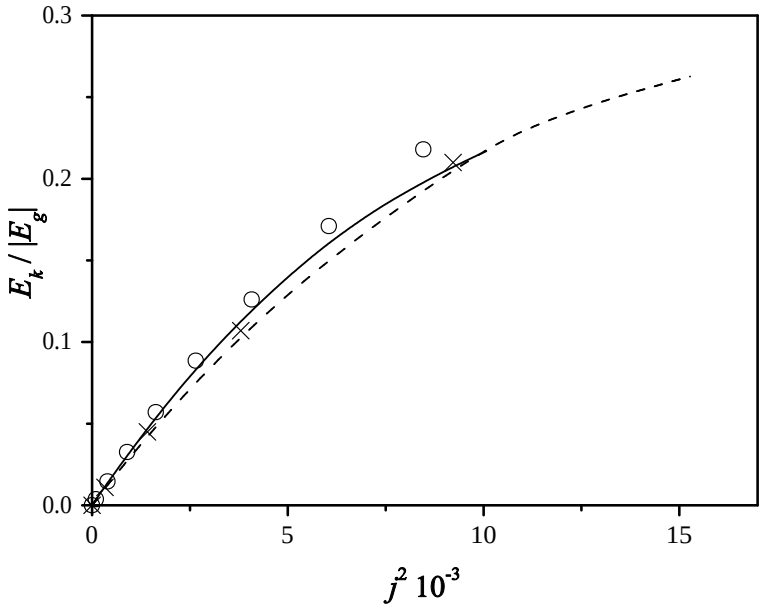

Figure 3.13: The $\beta(j^2)$ for v-const rotation law with $A = 0.2R_0$ (dashed, crosses) and $A = 0.02R_0$ (solid, circles), where lines refers to [7] and symbols refers to our formula with ΔC from (3.51). In this case we have good quantitative agreement with numerical results in both cases up to $\beta \simeq 0.1$.

E_{tot}) with numerical results for the entire range of rotation strength covered by both methods. The most extreme case ($A = 0.02$) also behaves well. The axis ratio (Fig. 3.14) however, clearly distinguishes between approximation and the precise solution. Results are quantitatively correct only for small rotation parameters, e.g $j^2 \ll 5 \cdot 10^{-3}$ i.e. $\beta \ll 0.1$.

Ω_0	ε	j^2	β	$-E_{tot}/E_0$	Virial test $\lvert Z\rvert$	ΔC
1.0	1.02	9.81×10^{-5}	0.004	0.30×10^{-5}	7×10^{-5}	0.01
2.0	1.09	3.94×10^{-4}	0.015	1.20×10^{-5}	1×10^{-4}	0.04
3.0	1.21	8.96×10^{-4}	0.03	2.75×10^{-5}	7×10^{-4}	0.09
4.0	1.41	1.63×10^{-3}	0.06	5.00×10^{-5}	5×10^{-4}	0.17
5.0	1.73	2.65×10^{-3}	0.09	8.09×10^{-5}	1×10^{-4}	0.27
6.0	2.24	4.08×10^{-3}	0.13	1.23×10^{-4}	3×10^{-4}	0.39
7.0	3.03	6.05×10^{-3}	0.17	1.77×10^{-4}	2×10^{-4}	0.55
8.0	4.60	8.46×10^{-3}	0.22	2.38×10^{-4}	3×10^{-4}	0.75

Table 3.6: Properties of v-const sequence for $A = 0.02R_0$.

3.9 Applicability of our formula

3.9.1 *Formula accuracy vs stability*

The Main conclusion from accuracy tests is that our very simple formula can give good global properties of a differentially rotating self-gravitating body, e.g. the total energy (3.68) or dimensionless angular momentum (3.70) for the stability parameter β in the range 0-0.05. But, according to stability analysis of [16], secular instability for highly deformed, with "toroidal" density stratification, objects may set at values as low as 0.038. From this point of view, our simple formula (3.33) is able to predict properties of differentially rotating objects with stability parameter range of all physically relevant (i.e. stable) objects. Nevertheless, final conclusion requires much more detailed accuracy testing, involving direct comparison of reference results* for a wide range of polytropic index n and for non-polytropic EOS.

3.9.2 *Failure for rigid rotation*

It is a bit surprising, that our formula works for differentially rotating bodies, producing accurate results, at least in small angular momentum limit, while completely fails for rigid rotation. The latter case is considered simpler and easier to handle. We wold like to propose criterion which may be used to determine when the formula fails.

Let us examine the behaviour of our formula (3.33) near the radius R_0 of non-rotating configuration described by an enthalpy distribution h_0:

$$h_1(r, z=0) \simeq h_0(R_0) - \Phi_c(R_0) - \Delta C + (r - R_0) \left.\frac{\partial(h_0 - \Phi_c - \Delta C)}{\partial r}\right|_{r=R_0}, \qquad (3.73)$$

where, of course, $h_0(R_0) = 0$. Now we can find an approximate equatorial radius R_1 of a rotating configuration from equation $h_1(R_1, 0) = 0$:

$$R_1 \simeq R_0 + \frac{1}{\kappa}\left[\Phi_c(R_0) + \Delta C\right], \qquad (3.74a)$$

*As a reference method, e.g. HSCF [11] numerical algorithm may be used.

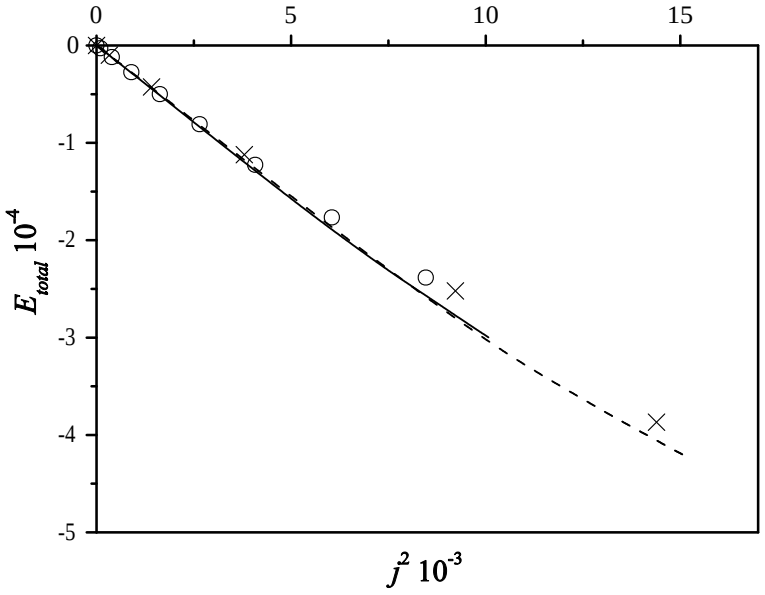

Figure 3.14: E_{tot} versus square of dimensionless angular momentum j^2. Symbols description is the same as in previous figure, Fig. 3.13.

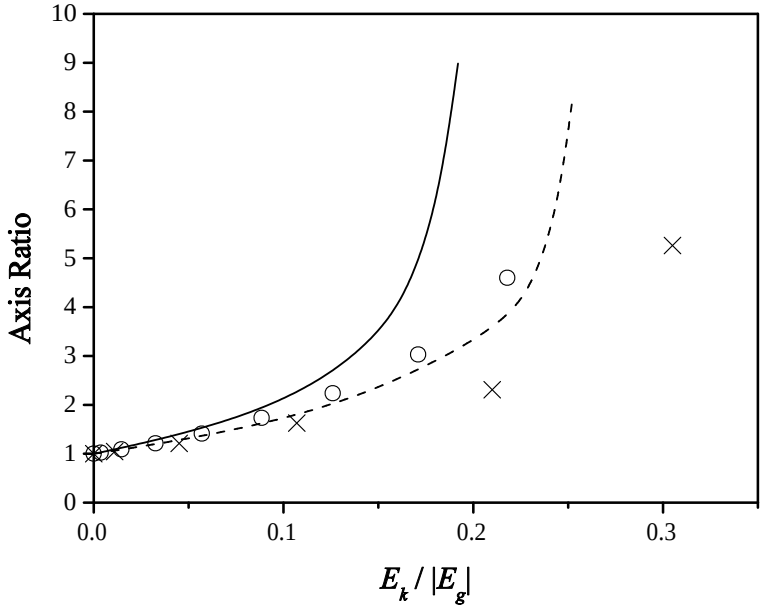

Figure 3.15: Axis ratio versus β for v-const rotation law. Symbols description is the same as in previous figures, Fig. 3.13 and Fig. 3.14.

$$\kappa = \left.\frac{\partial(h_0 - \Phi_c)}{\partial r}\right|_{r=R_0} = R_0\,\Omega(R_0)^2 + \left.\frac{\partial h_0}{\partial r}\right|_{r=R_0}, \tag{3.74b}$$

where $\partial\Phi_c/\partial r$ has been calculated using definition of the centrifugal potential (2.39). Both coefficient κ and expression $\Phi_c(R_0) + \Delta C$ are usually negative. From eq. (3.74a) we can see, that the radius R_1 of our approximation will be equal to R_0 only if ΔC is a boundary value $C^{(1)}$ from

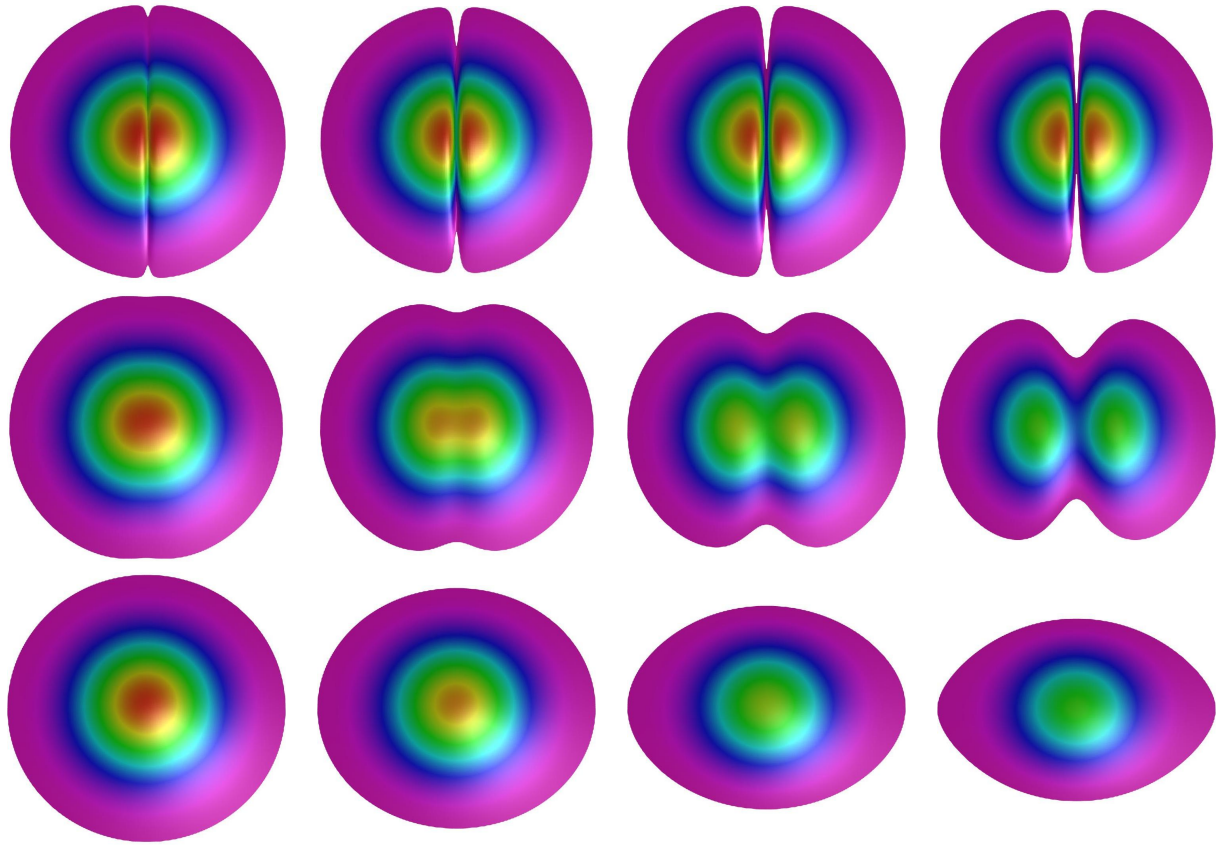

Figure 3.16: The enthalpy distributions for $n = 3/2$ polytropic sequence with j-const rotation law. Parameters of rotation are: upper row, from left: differentiability $A = 0.02R_0$; central angular velocity: $\Omega_0 = 75, 150, 200, 250$; middle row: differentiability $A = 0.2R_0$; central angular velocity: $\Omega_0 = 0.5, 1.0, 1.5, 2.0$; bottom row: differentiability $A = 2R_0$; central angular velocity: $\Omega_0 = 0.01, 0.02, 0.03, 0.035$.

Fig. 3.3. This does not lead to the best approximation (cf. TABLE 3.1, Fig. 3.7) – we have to use $\Delta C \neq -\Phi_c(R_0)$. Actually, in particular cases presented in this thesis (e.g. ΔC from virial test), $\Delta C > C^{(1)}$, and the radius of rotating configuration $R_1 > R_0$. In effect, differentiability parameter A, usually defined relatively to the radius of non-rotating configuration, is changed. In other words, we get accurate* solution, but for another differentiability parameter than defined initially. The strength of this effect is affected by both departure of ΔC from $-\Phi_c(R_0)$ and the value of parameter κ of linear function (3.74a). Difference $\Phi_c(R_0) - \Delta C$ increases with the rotation strength. For example, using centrifugal potential (3.56), and the ΔC from (3.72) we get

$$\Delta C + \Phi_c \simeq a\Omega^{2.2} - b\Omega^2, \tag{3.75}$$

but $b \gg a$ (cf. Fig. 3.7) and expression above is negative for Ω_0 of physically interesting range. Therefore the radius of the rotating configuration computed from our formula is always greater than R_0. The parameter κ is responsible for the departure rate. If $1/\kappa$ is very small the effect will also be small, even for strong rotation.

We are ready to discuss cases of differential and uniform rotation. For differential rotation, usually $\Omega(R_0) \simeq 0$ (cf. Fig. 3.5, 3.6). Therefore, $\kappa \simeq \partial h/\partial r|_{r=R_0}$ do not depend on the rotation strength, but only on EOS. Accordingly, the radius change is small for strong differential

*From e.g. virial test (3.50) point of view.

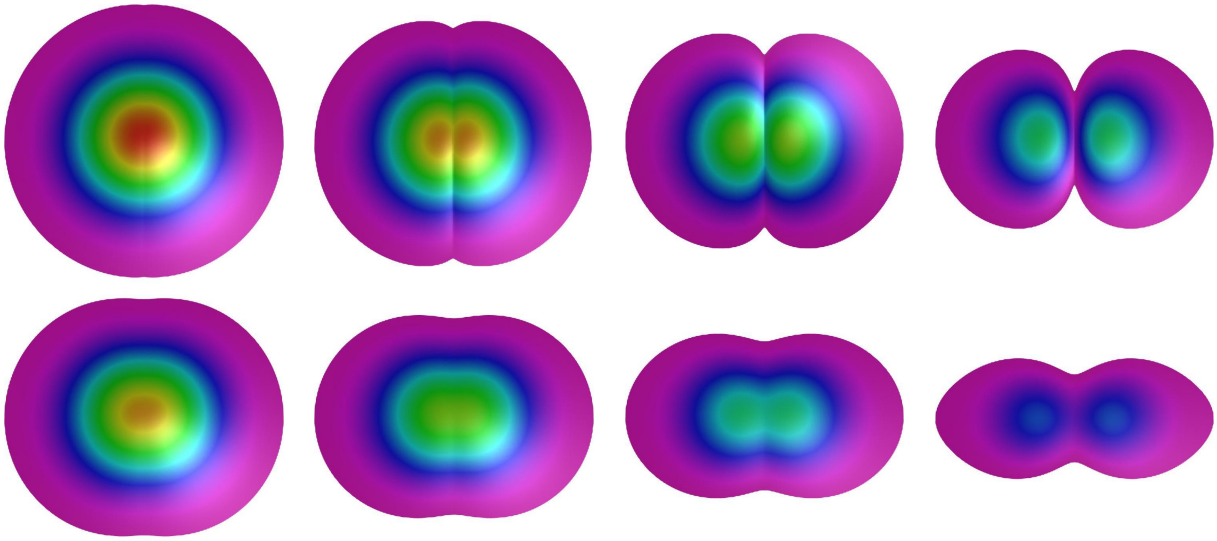

Figure 3.17: Properties of the enthalpy distributions for $n = 3/2$ polytropic sequence with v-const rotation law. Parameters of rotation are: upper row, from left: differentiability $A = 0.02R_0$; central angular velocity: $\Omega_0 = 1, 3, 5, 7$; lower row: differentiability $A = 0.2R_0$; central angular velocity: $\Omega_0 = 0.5, 0.75, 1.0, 1.25$.

rotation, if $\partial h/\partial r|_{r=R_0}$ is big, as for $n = 3/2$ polytropic case considered in previous sections.

For uniform rotation small increase in Ω_0 leads to significant decrease of $|\kappa|$. This leads to the differentiability parameter A change, and we are simply unable to compare our sequence of the rotating models with the sequence of constant parameters A.

Accordingly, we propose the following criterion:

$$\frac{\Phi_c(R_0) + \Delta C}{\kappa R_0} \ll 1 \tag{3.76}$$

for simple test if our formula is able to produce accurate results. This criterion simply rejects results with huge increase of the equatorial radius relative to the initial radius R_0. Definite answers regarding relevance of such a criterion, and related problem of corrections to differentiability parameter A, require further research.

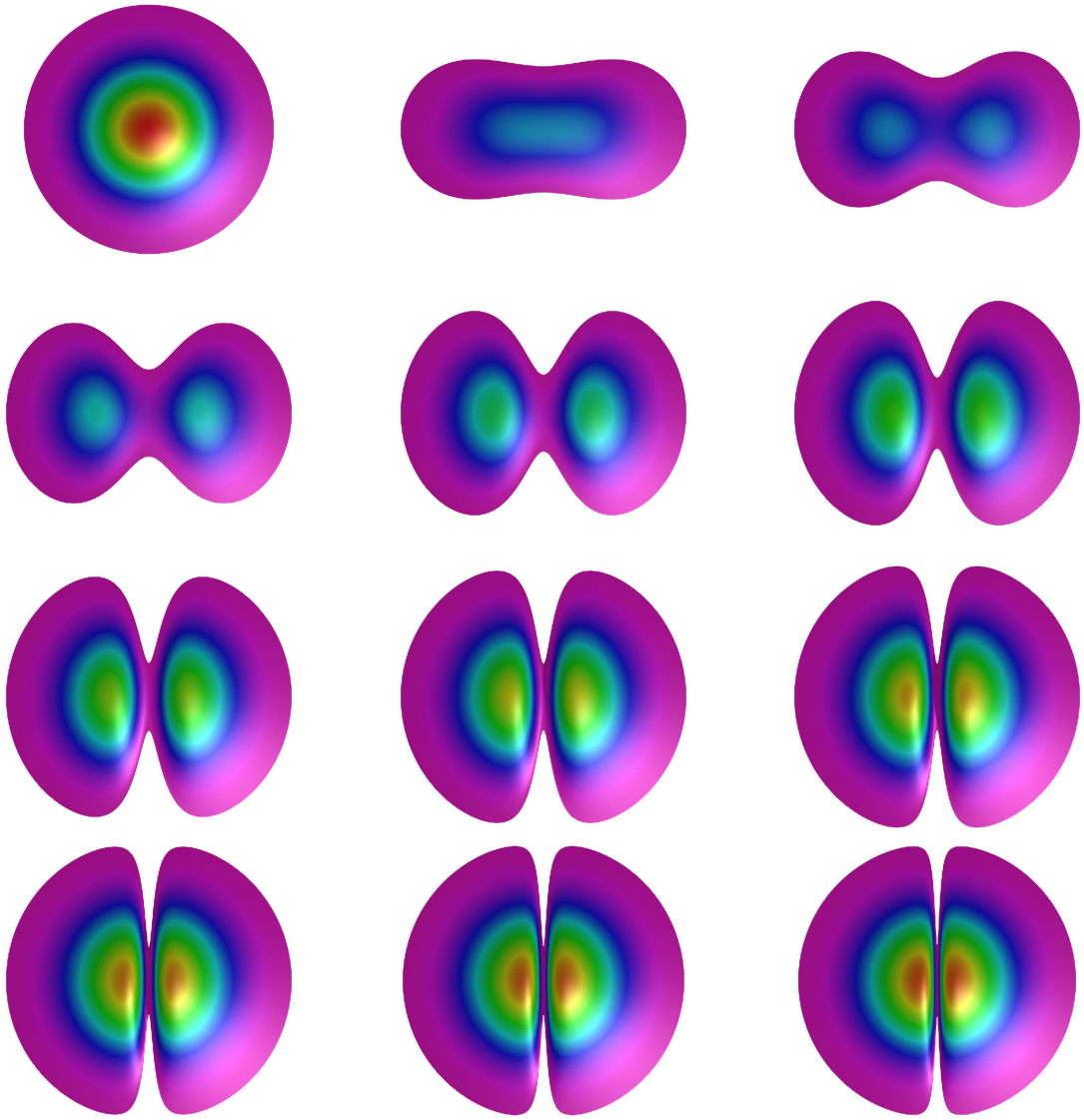

Figure 3.18: Another sequence of the $n = 3/2$ polytropic models with j-const rotation law. Sequence defined by $\Omega_0 A^2 = 0.1$. Non-rotating enthalpy distribution is presented in the upper-left corner. Values of Ω_0 and A are, from upper-left: (0.0,–), (1/4, 0.63), (1/2, 0.45), (1, 0.32), (2, 0.22), (4, 0.16), (8, 0.11), (16, 0.08), (32, 0.06), (64, 0.04), (128, 0.03) and (256, 0.02).

3.10 Conclusions and future prospects

3.10.1 *Importance of approximate formula*

The results of our thesis can be regarded as a next small step forward in our knowledge of the stellar rotation problems. Nowadays, these problems are usually attacked by means of numerical algorithms and simulations. Nevertheless, popularity of very simple idealized models like Maclaurin/Jacobi ellipsoids and Roche model, indicate need for such tools. Lack of deeper understanding, and difficulties with immediate application of numerical algorithms are possibly important reasons why we are still using approximate formulae in spite of their imperfection.

Our formula fall in a class of very simple tools. It is able to provide the internal structure of differentially rotating self-gravitating barotropes with acceptable accuracy. Iso-density contours of our $n = 3/2$ polytropic model are virtually identical to numerical results [21] if ro-

tation strength is small enough. From this formula which is barely sum of enthalpy, centrifugal potential and some constant value we have found such properties like polar "cusp," off-center density maximum and the "concave-hamburger" surface shape. Some important relationships, as e.g. kinetic to gravitational energy ratio β versus dimensionless angular momentum j^2 are obtained properly. Virial test, commonly used as a test for numerical results can be satisfied to an arbitrary accuracy within framework of our model. The main difficulty lays in proper choice of the constant value in the formula. The best results require numerical solving of equation involving multiple integrals. However, once calculated, these values are ready to use. Moreover, quantitative description of the internal structure does not require knowledge of that constant, as it only leads to redefinition of iso-enthalpy contours. In cases where zeroth-degree enthalpy and centrifugal potential are elementary functions, e.g. $n = 1$ polytrope with v-const or j-const angular velocity profile, the formula allows us to express result in a closed analytical form:

$$\rho_1(r,z) = \frac{\sin\sqrt{r^2+z^2}}{\sqrt{r^2+z^2}} + \frac{1}{2}\frac{\Omega_0^2 A^2 r^2}{1+r^2/A^2} - \frac{1}{2}\frac{\Omega_0^2 A^2 \pi^2}{1+\pi^2/A^2} \tag{3.77}$$

where $K = 1/2$, $4\pi G = 1$, $\rho_c = 1$, $\Omega(r) = \Omega_0/(1+r^2/A^2)$ and ΔC follows from eq. (3.34). Quality of the approximate formula above may be put in question, nevertheless no result of this kind was known for compressible body distorted due to differential rotation.

In general, the problem of differential rotation is considered to be very difficult. All results were obtained by means of numerical calculations. Our formula gives new insight in these results, showing that in huge part they are modification of enthalpy distribution due to centrifugal potential. It also reveals meaning of the enthalpy as a relevant physical quantity for description of rotating barotropic stars. This has a significant influence on numerical convergence rate, as noted by Eriguchi & Müller [7].

3.10.2 *Application of approximate results*

Our approximation may be used as an initial guess for initial algorithms. Usually (e.g for HSCF) it is enough to use flat initial distribution to start iteration, but possibly we may get faster convergence if we start from our formula. The method of Eriguchi & Müller, however, requires initial guess to be very close to the final result. This is achieved by subsequent calculations of a sequence of similar models, beginning with known non-rotating structure. Even if we are interested in just one rapidly rotating model, we have to calculate the entire sequence. It may significantly increase computational power required. If one uses our approximate rotating structure, the algorithm hopefully will start successfully. Our formula may be also used as a fit to data produced by numerical methods for later use in a much more convenient form.

3.10.3 *Area of further research*

Derivation and analysis of our formula provided new insight in structure of differentially rotating self-gravitating bodies. It also has opened new problems and questions.

Our analysis has shown that virial test can be satisfied to an arbitrary accuracy. It is also true for extremely distorted approximate models. These models are not in equilibrium, as we can infer from e.g. $\beta(j^2)$ comparison to the results of [7]. This is not surprise, as virial test is necessary, but not sufficient condition for equilibrium. Therefore, we could consider also other tests e.g. direct comparison to numerically derived structure. This requires development of appropriate software and least-square fits of our formula to computed results. This way we will

also check out quality of our formula as a fitting tool, and possibly will find further methods of the formula improvement.

Another very interesting possibility is the power law dependence of ΔC eq. (3.72) satisfying the virial theorem. The exponent $\alpha \simeq 2.2$ has been found for $n = 3/2$ polytrope with j-const rotation law. It should be examined if power law can be used in other cases. Possibly the exponent α has a universal character.

Continuation of the Lane-Emden functions to negative values leads to a small ambiguity. Nevertheless, some of the rotating model properties, namely the shape of the surface may be sensitive to particular choice of the continuation method, e.g. the axis ratio of our models could then possibly be adjusted to correct apparent underestimation of this important quantity.

Failure for uniform rotation may a be result of the differentiability change, due to increase in the radius of rotating configuration. This may also affect structure of differentially rotating models. Therefore our results could be corrected to reduce influence of this effect. Potentially, our formula could be improved this way to become relevant also for homogeneous rotation.

APPENDIX A: LINEAR INTEGRAL EQUATIONS

Consider linear integral equation:

$$f(x) = \int_a^b K(x,y)\, f(y)\, dy + g(x), \tag{A-1}$$

This equation is classified as a linear Fredholm's integral equation of the second kind. Let us define linear (integral) operator $\mathcal{K}$:

$$\mathcal{K}(f) = \int_a^b K(x,y)\, f(y)\, dy, \tag{A-2}$$

and the operator $\mathcal{H}$:

$$\mathcal{H}(f) = \mathcal{K}(f) + g. \tag{A-3}$$

We can write the Fredholm's equation as:

$$f = \mathcal{H}(f). \tag{A-4}$$

Series of the form:

$$f_k(x) = \sum_{n=0}^{k} \mathcal{K}^n g(x) \tag{A-5}$$

is referred to as the von Neumann series. Partial sum of the von Neumann series can be also calculated from recursive expression:

$$f_{k+1} = \mathcal{H}(f_k), \tag{A-6}$$

with $f_0 \equiv 0$, $f_1 = g(x)$, etc.

The following theorem can be proved: If the function $g(x)$ is integrable in the range $[a,b]$, and:

$$\max_{\substack{a<x<b \\ a<y<b}} |K(x,y)| < \frac{1}{b-a}, \tag{A-7}$$

then the function f, such that

$$f(x) = \sum_{n=0}^{\infty} \mathcal{K}^n g(x) \tag{A-8}$$

is a unique integrable solution to the Fredholm's equation of the second kind (A-1).

In terms of the recursive expression, we may write this solution as:

$$f(x) = \lim_{k\to\infty} f_k(x), \tag{A-9}$$

where f_k is defined in (A-6).

More information on integral equations can be found in e.g. Ref. [25].

APPENDIX B: LANE-EMDEN FUNCTIONS

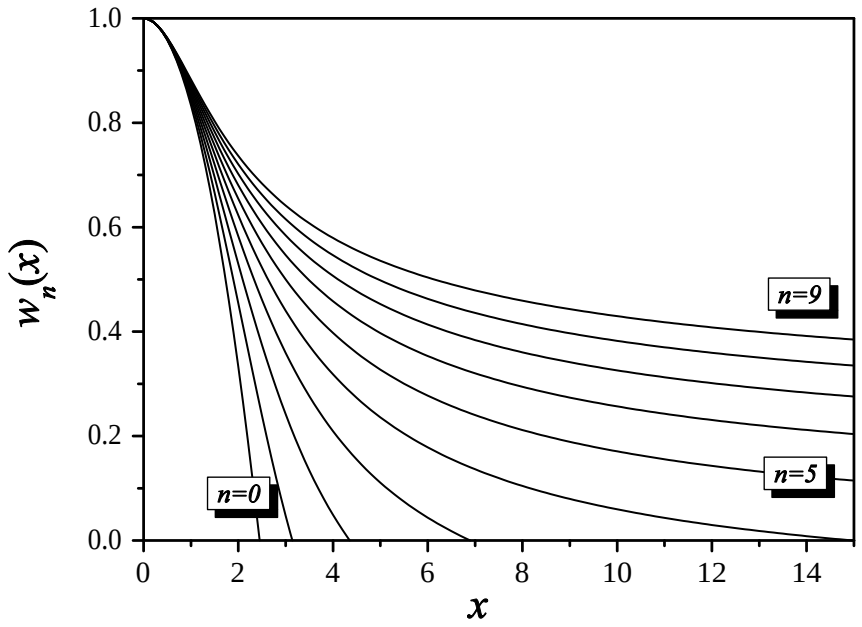

Figure B-1: Lane-Emden functions $w_n(x)$ for $n = 0, 1, 2, 3, 4, 5, 6, 7, 8, 9$. Let note increasing with polytropic index the radius R_0 of a configuration. For $n \geq 5$ radius is infinite.

Structure of non-rotating polytropes is a standard approximation for real stars. This is also required for our approximate formula as an initial zeroth-order approximation for rotating objects. We begin with the equation (2.42) without rotation ($\Phi_c \equiv 0$):

$$h + \Phi_g = C. \tag{B-1}$$

Laplacian of the equation (B-1), according to Poisson equation (2.14) is:

$$\Delta h + 4\pi G\rho = 0. \tag{B-2}$$

EOS (3.61) gives the relation (3.63) between enthalpy and density. By inverting this relation we get:

$$\Delta h + 4\pi G \left(\frac{\gamma - 1}{K\gamma}\right)^n h^n = 0. \tag{B-3}$$

Introducing new independent variable $\mathbf{x}$ and a function $w(x)$:

$$\mathbf{x} = \mathbf{r} \sqrt{4\pi G \left(\frac{\gamma - 1}{K\gamma}\right)^n} \, h_c^{(n-1)/2}, \tag{B-4a}$$

$$h(x) = h_c \, w(x), \tag{B-4b}$$

where h_c is the central enthalpy, we get:

$$\Delta w + w^n = 0 \tag{B-5}$$

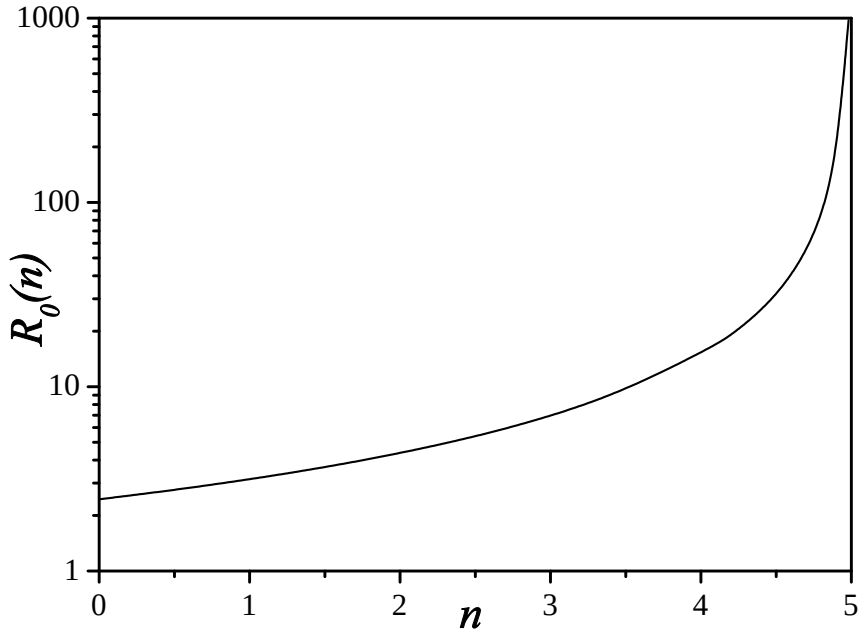

Figure B-2: Radius of a Lane-Emden configuration, i.e. locus of Lane-Emden zero-points ($w(R_0) = 0$) as a function of polytropic index $R_0(n)$. If n approaches $n = 5$ (i.e. $p \sim \rho^{6/5}$), the radius goes to infinity.

For spherical symmetry, the Laplace operator becomes:

$$\Delta_x = \frac{1}{x^2}\frac{\partial}{\partial x}\left(x^2\frac{\partial}{\partial\, x}\right). \tag{B-6}$$

Finally, we get the famous Lane-Emden equation:

$$\frac{1}{x^2}\frac{\partial}{\partial x}\left(x^2\frac{\partial w}{\partial\, x}\right) + w^n = 0 \tag{B-7}$$

Solutions of eq. (B-7) with initial conditions:

$$w(0) = 1, \quad w^{'}(0) = 0, \tag{B-8}$$

define a set of special functions $w_n(x)$ referred to as Lane-Emden functions.

APPENDIX C: CALCULATING GLOBAL QUANTITIES

In this appendix we will address some technical details concerning calculations of integrals used in the text. We encounter integrals I_1, I_2 of the following form:

$$I_1 = \int_0^{2\pi} \frac{d\,\phi}{\sqrt{(r'\sin\phi' - r\sin\phi)^2 + (r'\cos\phi' - r\cos\phi)^2 + (z'-z)^2}}, \tag{C-1}$$

$$I_2 = \int_0^{2\pi}\int_0^{2\pi} \frac{d\phi\; d\phi'}{\sqrt{(r'\sin\phi' - r\sin\phi)^2 + (r'\cos\phi' - r\cos\phi)^2 + (z'-z)^2}}. \tag{C-2}$$

These integrals are results of $1/|\mathbf{r}-\mathbf{r}'|$ term in the Newtonian gravitational energy and gravitational potential. Both of the integrals I_1, I_2 can be computed analytically, using the special function

$$f(\varkappa) = \int_0^{\pi/2} \frac{d\psi}{\sqrt{1+\varkappa\sin^2\psi}}, \tag{C-3}$$

and the result is:

$$I_1 = \frac{4\,f(p)}{\sqrt{(r-r')^2+(z-z')^2}}, \tag{C-4}$$

$$I_2 = \frac{8\,\pi\,f(p)}{\sqrt{(r-r')^2+(z-z')^2}}, \tag{C-5}$$

where:

$$p = \frac{4rr'}{(r-r')^2+(z-z')^2}. \tag{C-6}$$

Proof:
We rewrite denominator of the I_1 in the form:

$$I_1 = \int_0^{2\pi} \frac{d\,\phi}{\sqrt{(r'^2 + r^2 - 2rr'\cos(\phi-\phi') + (z'-z)^2}}.$$

After variable change according to:

$$\frac{\phi-\phi'}{2} = \psi, \quad cos(\phi-\phi') = 1 - 2\,\sin^2\psi, \quad d\phi' = -2\,d\psi$$

using definition (C-6), we get:

$$I_1 = \frac{2}{\sqrt{(r-r')^2+(z-z')^2}} \int_{\phi/2-\pi}^{\phi/2} \frac{d\psi}{\sqrt{1+p\,\sin^2\psi}}.$$

Integrand is a periodic function with the period $T = \pi$. Definite integrals of any periodic function $f(x)$ over closed interval $[\varkappa, \varkappa+T]$ do not depend on $\varkappa$:

$$\frac{d}{d\varkappa}\int_{\varkappa}^{\varkappa+T} f(x)\,dx = \frac{d}{d\varkappa}\left(F(\varkappa+T) - F(\varkappa)\right) = f(\varkappa+T) - f(\varkappa) = 0,$$

where $F(x)$ is primitive function ($F^{'} = f$) and, according to the periodic character of the function $f(x)$, of course, $f(\varkappa + T) = f(\varkappa)$. Accordingly, I_1 does not depend on ϕ. Using $\phi = \pi/2$ we get:

$$2 \int\limits_{-\pi/2}^{\pi/2} \frac{d\psi}{\sqrt{1 + p\, \sin^2 \psi}} = 4 \int\limits_{0}^{\pi/2} \frac{d\psi}{\sqrt{1 + p\, \sin^2 \psi}},$$

what ends the proof. As the integral I_1 does not depend on ϕ, we immediately get $I_2 = 2\pi\, I_1$.

The function f is directly related to elliptic integrals. Unfortunately, two (at least) definitions for elliptic functions are in use. Usually, one defines elliptic integral of the first kind as:

$$F(k, \phi) = \int\limits_{0}^{\phi} \frac{d\psi}{\sqrt{1 - k^2 \sin^2 \psi}}, \tag{C-7}$$

and complete elliptic integral as:

$$E(k) = F\left(k, \frac{\pi}{2}\right) = \int\limits_{0}^{\pi/2} \frac{d\psi}{\sqrt{1 - k^2 \sin^2 \psi}}. \tag{C-8}$$

Sometimes these functions are defined by:

$$\widetilde{F}(m, \phi) = \int\limits_{0}^{\phi} \frac{d\psi}{\sqrt{1 - m \sin^2 \psi}}, \tag{C-9}$$

and complete elliptic integral as:

$$\widetilde{E}(m) = \widetilde{F}(m, \frac{\pi}{2}) = \int\limits_{0}^{\pi/2} \frac{d\psi}{\sqrt{1 - m \sin^2 \psi}}. \tag{C-10}$$

We may easily convert $\widetilde{F}(m, \phi), \widetilde{E}(m)$ to $F(k, \phi), E(k)$ simply by substitution $m = k^2$. Our function f becomes, by the first definition

$$f(p) = E(i\sqrt{p}), \tag{C-11}$$

but, from the second definition:

$$f(p) = \widetilde{E}(-p). \tag{C-12}$$

The following identity is very useful in calculations involving integrals similar to I_1 and I_2:

$$\frac{1}{2}\left[F\left(\frac{\phi}{2}, ik\right) - F\left(\frac{\phi}{2} - \pi, ik\right)\right] = E(ik) \tag{C-13}$$

One should carefully check out definitions of elliptic integrals before using foregoing expressions.

Now we write explicitly formulae for axially symmetric density distributions, i.e. $\rho = \rho(r, z)$. Gravitational energy of the self-gravitating axially symmetric body is:

$$E_g = 4\,\pi\, G \int\limits_{0}^{R} \int\limits_{-R}^{R} \int\limits_{0}^{R} \int\limits_{-R}^{R} \frac{f(p)\ \rho(r, z)\ \rho(r^{'}, z^{'})}{\sqrt{(r - r^{'})^2 + (z - z^{'})^2}} r\, dr\, dz\, r^{'}\, dr^{'}\, dz^{'}, \tag{C-14}$$

where p is defined in (C-6), and the function $f(p)$ is simply the complete elliptic function (C-12, C-11), according to relevant definition. R should be chosen big enough to contain density distribution $\rho(r,z)$. The area outside the surface $\rho(r,z)=0$ is empty, and does not contribute to gravitational energy E_g. This may be ensured by adding to the integrand of (C-14) the following expression:

$$\theta\big(\rho(r,z)\big)\;\theta\big(\rho(r^{'},z^{'})\big),$$

where θ is the unit step function (3.13). Integral E_g is calculated numerically with use of Monte Carlo method, to avoid problems with singularities of the integrand.

Other integrals, i.e. the total angular momentum, kinetic energy, mass and internal energy in cylindrical coordinates are straightforward. The angular momentum is given by:

$$J = 2\,\pi \int_{0}^{R}\int_{-R}^{R} \rho(r,z)\,\Omega(r)\,r^3 dr\,dz. \tag{C-15}$$

The kinetic (rotational) energy is:

$$E_k = \pi \int_{0}^{R}\int_{-R}^{R} \rho(r,z)\,\Omega(r)^2\,r^3 dr\,dz. \tag{C-16}$$

The total mass is:

$$M = 2\,\pi \int_{0}^{R}\int_{-R}^{R} \rho(r,z)\,r\,dr\,dz. \tag{C-17}$$

These integrals are calculated numerically. Any method may be used here, as integrands are just finite, smooth functions of two variables. Values of J, E_k, M and E_g are required to calculate virial test parameter Z and dimensionless global quantities e.g. $E_k/|E_g|$.

APPENDIX D: STABILITY OF THE ROTATING OBJECTS

From our approximate formula (and by other methods) we are able to compute structure of differentially rotating self-gravitating bodies. Actually, only a fraction of them is of (astro)physical interest – real world objects, in contrast to purely mathematical solution, have to be *stable*. All examples given in this thesis are chosen to satisfy stability conditions.

We now list stability criteria relevant to discussion in our thesis.

The global stability

For non-rotating spherically symmetric stars, with polytropic EOS (3.61) and Newtonian gravity, the following criteria holds:

- If polytropic exponent $\gamma > \gamma_{cr} = \frac{4}{3}$ (equivalently if polytropic *index* $n < 3$) then the object is *stable*
- If polytropic exponent $\gamma < \gamma_{cr} = \frac{4}{3}$ (equivalently if polytropic *index* $n > 3$) then the object is *unstable*
- If polytropic exponent $\gamma = \gamma_{cr} = \frac{4}{3}$ (equivalently if polytropic *index* $n = 3$) then the object is *marginally stable*.

Here we have defined the critical value of γ:

$$\gamma_{cr} = \frac{4}{3} \tag{D-1}$$

Rotation tends to stabilize object against collapse. The problem of the stability of rotating (especially differentially rotating) bodies has not yet been fully solved. However, the following criterion derived for uniformly rotating polytropes is widely used. We define the effective polytropic exponent:

$$\gamma_{eff} = \gamma_{cr} \frac{1 - \frac{5}{2}\beta}{1 - 2\beta}, \tag{D-2}$$

where β is the rotational kinetic energy to gravitational energy ratio (3.71). The value of β is never greater than $1/2$ (see text below); $\beta = 2/5 = 0.4$ is also highly unlikely, as e.g. dynamical instability limit for Maclaurin spheroid is 0.2738. Therefore, from (D-2), the critical polytropic exponent is always reduced if rotation is present. Accordingly, stable rotating objects with polytropic index $n > 3$ ($\gamma < 4/3$) may exist.

Stability of angular momentum distribution

In differentially rotating stars we have to answer a question, whether prescribed angular velocity profiles leads to a stable object.

It can be proved, that in stable object the angular momentum per unit mass has to decrease outward. This is the Solberg criterion. We may write this stability condition as:

$$\frac{\partial}{\partial r}\left(r^4\,\Omega(r,z)^2\right) > 0. \tag{D-3}$$

As an example we check out if the angular velocity profiles used in our thesis are stable with respect to the Solberg criterion. Let the angular velocity be:

$$\Omega(r) = \frac{\Omega_0}{1 + (r/A)^\varsigma} \tag{D-4}$$

The Solberg criterion requires:

$$\frac{\partial}{\partial r}\left[r^4\,\Omega(r,z)^2\right] = \Omega(r)^3\,2\,\frac{r^3}{\Omega_0}\left[2+(2-\zeta)\,\left(\frac{r}{A}\right)^{\zeta}\right] > 0. \tag{D-5}$$

As we can see, if $\zeta \leq 2$ then our rotation law is stable against small perturbations for any differentiability A. If $\zeta > 2$ then, taking into account maximum radius of a star R_0 (i.e. the equatorial radius) we get:

$$A > R_0\,(\zeta/2-1)^{1/\zeta} \sim R_0 \tag{D-6}$$

because expression $(\zeta/2-1)^{1/\zeta}$ is of the order of 1 for $\zeta > 2$. Differentiability A cannot be too small ($A << 1$), i.e. we are unable to concentrate too much angular momentum in a central region of a star. Physical intuition as to this instability is simple: centrifugal force in the central region is strong enough to remove matter (and thus angular momentum) from the core.

Secular & dynamical instability

It is intuitively obvious, that rotating body cannot possess too much angular momentum, because like for solid rotating bodies, centrifugal forces tend to disrupt it. What is then maximum amount of rotation allowed? Almost 300 hundred years ago Maclaurin [20] work raised this question, and the problem is still investigated [2, 16].

Various combinations of physical quantities may be used as rotation strength indicator. The most widely used by astrophysicists is the ratio of the total kinetic energy E_k and modulus of the gravitational energy E_g, denoted by β (3.71). From virial theorem (3.47) we can get the following estimation:

$$\beta = \frac{E_k}{|E_g|} = \frac{1}{2} - \frac{3}{2}\frac{\int p\,d^3\mathbf{r}}{|E_g|} \leq \frac{1}{2}, \tag{D-7}$$

because pressure is non-negative quantity. Actually, it is impossible to reach the value of $\beta = 0.5$, because dynamical instability is encountered at 0.27 or less.

Stability analysis for uniformly rotating bodies leads to the following conclusions. For polytropic index $n < 0.8$, behaviour of rotating compressible body closely resembles rotating constant density bodies. Therefore, stability analysis of the Maclaurin spheroids and Jacobi ellipsoids is representative. Namely, if $\beta < 0.1375$, rotating body is stable. Beyond $\beta = 0.1375$ at least two possible equilibria exist: the axially symmetric Maclaurin spheroid and the triaxial Jacobi ellipsoid. As Jacobi ellipsoid for $\beta > 0.1375$ has lower total mechanical energy, so-called secular instability is possible. This leads to transition of axially symmetric configuration into non-axisymmetric one, if dissipative processes are present, e.g. viscosity. If dissipative process do not operate or its strength is small, then Maclaurin spheroid can store as much as $E_k = 0.27|E_g|$ of kinetic energy. Triaxial bodies are dynamically unstable at significantly lower β of 0.16.

Completely different behaviour is found for centrally condensed bodies, i.e. with polytropic index of $n > 0.8$. Such uniformly rotating barotrope is unable to store large rotational kinetic energy, because centrifugal force exceeds gravitational force well before any instability could occur. This leads rather to equatorial mass loss, not a global instability of a body. Situation becomes much different if, like in our thesis, differential rotation is taken into account. Stability analysis in that case is still in progress, and generally requires dynamical simulations of rotating configurations. Both secular and dynamical instability may set at significantly lower values, compared to uniform, rigidly rotating bodies. For example articles [2, 16] report the onset of secular instability at $\beta = 0.04$ and dynamical instability at $\beta = 0.14$. Nevertheless, too much

angular momentum in the central region may lead to violation of Solberg and Høiland criteria (D-3).

General rotating star may be also subject of other instabilities, e.g. related to energy transfer and mixing, but they are beyond the scope of our simple barotropic models. Reader is referred to textbook of Tassoul [29] and to Sect. 2.3 of [13] and references therein.

INDEX

REFERENCES

[1] I. N. Bronsztejn, K. A. Siemiendiajew, *Matematyka, poradnik encyklopedyczny*, PWN.

[2] J. N. Centrella et. al., *Astrophysical Journal* **550** (2001) L193.

[3] S. Chandrasekhar, *Hydrodynamic and Hydromagnetic Stability*, Dover Publications Inc., 1981.

[4] P. Dive, Bull. Sci. Math., **76** (1952) 38.

[5] Y. Eriguchi, Publ. Astron. Soc. Japan **30** (1978) 507.

[6] Y. Eriguchi, Progress of Theoretical Physics, **64** (1980) p. 2009.

[7] Y. Eriguchi and E. Müller 1985 Astronomy&Astrophysics, **146**, 260

[8] T. Fukushima, Y. Eriguchi, D. Sugimoto, G. S. Bisnovatyi-Kogan, Progress of Theoretical Physics **63** (1980) p. 1957.

[9] Galileo Galilei, *Dialogue Concerning the Two Chief World Systems - Ptolemaic & Copernican*, 1632.

[10] Y. Eriguchi, I. Hachisu, Progress of Theoretical Physics, **67** (1982) p. 844.

[11] I. Hachisu, Astrophysical Journal Supplement Series, **61** (1986) 479.

[12] A. Hammerstein, 1930 Acta Mathematica, 54, 117.

[13] A. Heger, N. Langer and S. E. Woosley, *Presupernova Evolution of Rotating Massive Stars I: Numerical Method and Evolution of the Internal Stellar Structure*, Astrophysical Journal, **528** (2000) 36.

[14] A. Heger, N. Langer and S. E. Woosley, *Presupernova Evolution of Rotating Massive Stars II: Evolution of the Surface Properties*, Astrophysical Journal, **544** (2000) 1016.

[15] A. Heger, S. E. Woosley, N. Langer, H. C. Spruit *Presupernova Evolution of Rotating Massive Stars and the Rotation Rate of Pulsars* astro-ph/0301374 (2002, Proc. IAU215: Stellar Rotation, eds. A. Maeder, P. Eenens)

[16] J. N. Imamura, R. H. Durisen, *The Astrophysical Journal*, **549**, 1062–1075, (2001).

[17] R. Kippenhahn, A. Weigert, 1994, Stellar Structure and Evolution. Springer-Verlag p. 176

[18] L. D. Landau, E. M. Lifszyc, *Hydrodynamika*, wydanie 3, PWN Warszawa, 1994.

[19] N. R. Lebovitz, *Rotating fluid masses*, ARA&A **5** (1967) 465.

[20] C. Maclaurin, *A treatise of fluxions*, Printed by T. W. & T. Ruddimans, Edinburgh, 1742.

[21] A. Odrzywołek, *Analytical approximation for the structure of differentially rotating barotropes*, MNRAS **345** (2003) 497.

[22] A. Odrzywołek et. al., *Core-Collapse Supernova Mechanism - Importance of Rotation*, Acta Physica Polonica B **34** (2003) 2791.

[23] K. Oka et. al., Astronomy&Astrophysics **394** (2002) 115.

[24] J. P. Ostriker, J. W.-K. Mark, Astrophysical Journal **151** (1968) 1075.

[25] A. Piskorek, *Rownania całkowe*, WNT, Warszawa, 1997.

[26] M. Rampp, E. Müller, M. Ruffert, Astronomy&Astrophysics **332** (1998) 969.

[27] R. Stoeckley, *Polytropic models with fast, non-uniform rotation*, Astrophysical Journal **142** (1965) 208.

[28] J-L. Tassoul, *Theory of Rotating Stars*, Princeton University Press, 1978.

[29] J-L. Tassoul, *Stellar Rotation*, Cambridge University Press, 2000.